Beacon-analysis

Jeroen Kersten

august 21, 2012

Preface

This thesis is the result of my Bachelor internship at the department of Experimental High Energy Physics of the Institute of Mathematics, Astrophysics and Particle Physics at the Radboud University of Nijmegen. I would like to thank Stefan Grebe, Harm Schoorlemmer, Stefan Jansen, Guus van Aar and my supervisor Charles Timmermans.

Contents

1 Introduction

Every minute of the day the Earth gets bombarded with high-energetic particles from outer space. These particles enter our atmosphere and induce showers of secondary particles. We can study and measure these particles in various ways. One way to measure these particles is by using radio detectors. These detectors measure the electro-magnetic signal that is produced by the induced showers. To perform precise measurements of the shower and to reduce uncertainties of such a measurement as much as possible, it is important to calibrate these detectors relative to each other.

That is why I am doing an analysis on the beacon data. The beacon is a radio-antenna that is transmitting sinuslike electromagnetic signals on different frequencies. This study is about how we can use these signals transmitted by the beacon in order to improve the reconstruction of the energy and the direction of the shower. This is important because we want to make good estimates about the composition, energy and direction of the primary particle. In this study, I am using of the amplitude and the phase of the sinuslike signals that are transmitted by the beacon and are received by the radio detectors.

1.1 Cosmic rays and extensive air showers

Cosmic rays are high-energetic particles from outer space. These particles can be protons (90%), helium nuclei, iron nuclei, electrons etc. If a high energetic particle enters the atmosphere of the Earth (the primary particle) and collides with a nulceus in the atmosphere, secondary particles (electrons, photons, muons etc.) are created. These secondary particles on their turn, interact in different ways with other particles in the atmosphere and create new secondary particles. This process continues until there are no more secondary particles with an energy high enough to create other particles. This shower of particles, that can exist of billions of particles, is called an extensive air shower (EAS). EAS's with energies above 10^{18}eV can produce a footprint on the Earth, in which secondary particles can still be measured, of about 25 km^2.

Cosmic rays have energies between 10^8 eV and 10^{21} eV. The origin and acceleration of these particles originate from different sources. For example, particles can get ejected in a supernova explosion or in a solar wind. They get accelerated by all kinds of magnetic fields in space, for example the magnetic field around the sun, in and around solar winds and supernova remnants. The known sources of acceleration in space can explain the energy of cosmic rays up to 10^{16} eV. However, sometimes we observe cosmic rays of 10^{19} eV. We do not know what the source of these ultra high-energetic particles is. In the quest of finding out what kind of sources can explain these high energies, it is important to study these cosmic rays and to determine their energy, direction and composition.

Cosmic rays with energies above 10^{16}eV are rare, about 1 particle per m^2 per year. So we need a very large detector to measure enough of these particles in a short time span. We cannot build such a detector above the atmosphere to measure them directly, so we need to study cosmic rays by studying the EAS's.[1]

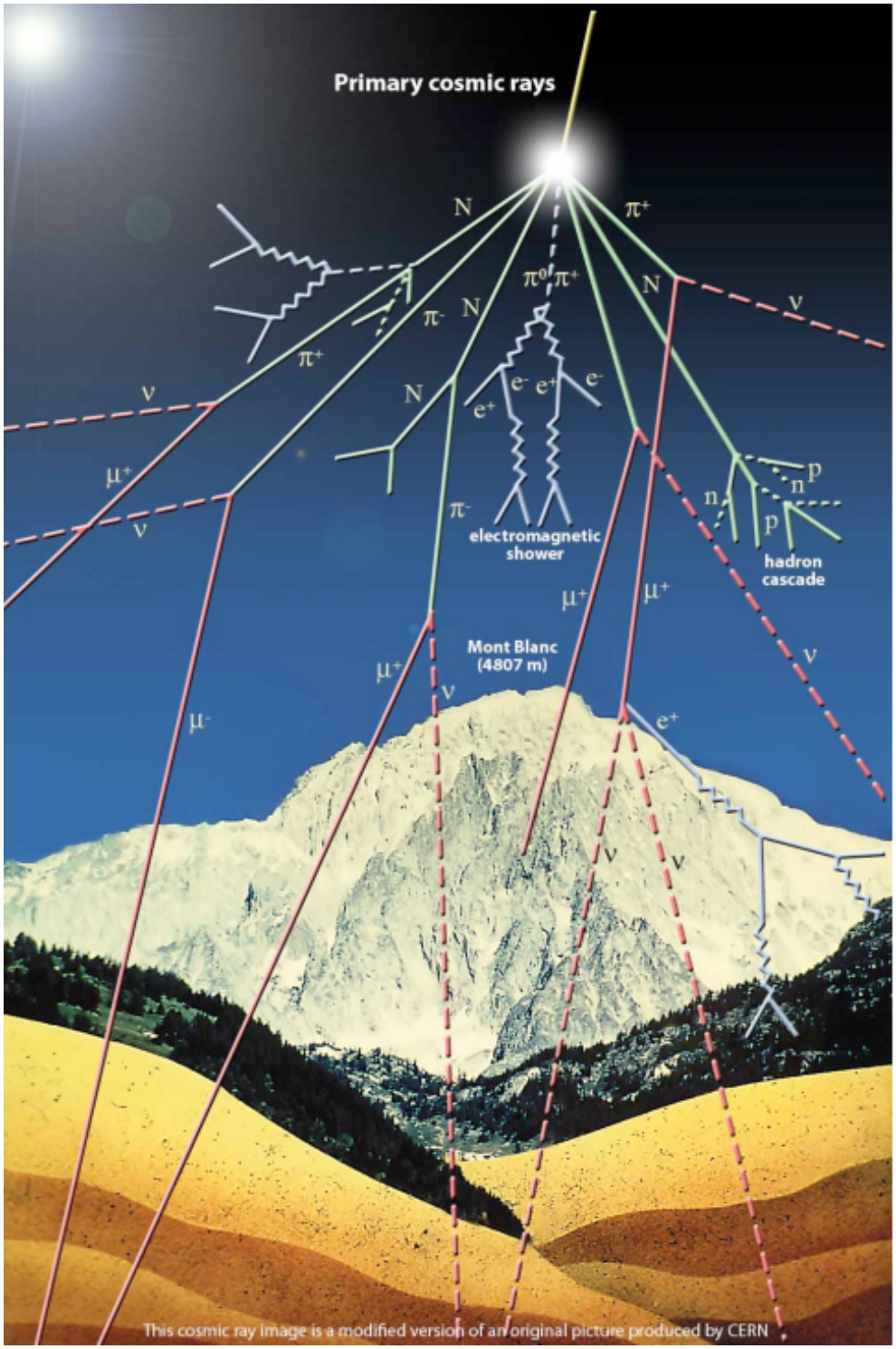

Figure 1.1: An extensive air shower, a primary particle enters the atmosphere of the Earth. It collides with a particle in the atmosphere and this causes a shower of secondary particles. Different processes play a role in the creation of these secundairy particles (A secondary particle can collide and create new particles but new particles can also be created by pair-pair production and a lot of other reactions).[2]

1.2 The Pierre Auger Observatory

The Pierre Auger Observatory is built to detect cosmic rays with energies above 10^{18} eV. These particles do not hit the Earth very often, only about 1 time per year per km^2, which is why this observatory covers a surface of 3000 km^2. The Pierre Auger observatory is located on the southern hemisphere near the city Malargüe in Mendoza, Argentina. It is named after Pierre Victor Auger, the first person who observed an extensive air shower that was produced by high-energetic cosmic rays. The observatory uses different types of detection methods to measure EAS's. A map of the observatory is shown in figure 1.2.

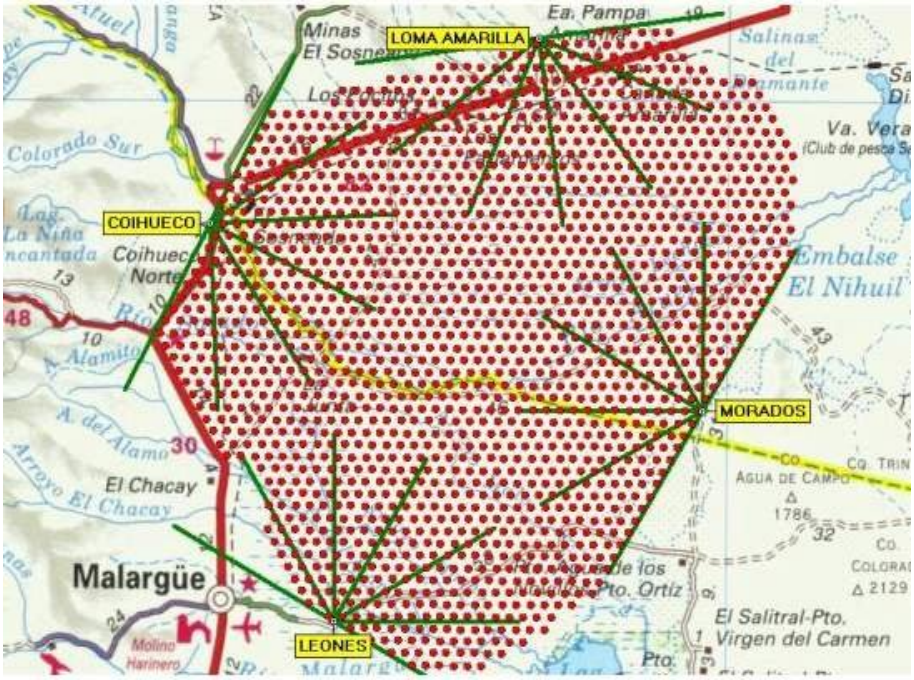

Figure 1.2: The Pierre Auger Observatory, covers a surface of 3000 km^2. The red points indicate the surface detectors and the green lines indicate the field of view of the fluorescence detectors.[3]

1.3 Surface en fluorescence detectors

There are 1600 surface detectors distributed over the area, which are separated from each other by 1.5 km. A surface detector consists of a water tank filled with 12.000 liter of water. Three photomultiplier tubes are mounted inside the tank, where it is completely dark. If particles from an EAS pass through the water they emit Cherenkov radiation. This radiation arises if a particle travels faster than the speed of light in water. The photomultiplier tubes measure this radiation and register it as a signal. If a signal gets measured in three or more surface detectors we can use the detection time and signal strenght to determine the direction and energy of an EAS.[4]

The secondary particles of the EAS also interact with the nitrogen in the atmosphere. A charged particle can be the cause that a nitrogen-atom gets into an excited state. If this atom falls back to its ground state, the atom loses energy and this energy gets emitted as photon, in the ultraviolet region of the spectrum. The fluorescence detectors are designed in such a way that they measure this light. They consist of mirrors and sensitive photomultiplier tubes and can detect EAS's with energies above 10^{18}eV up to 15 km away. This detector measures the development of the EAS from which we determine the composition of the EAS. The fluorescence detector works like a calorimeter and thus can also measure the energy of the EAS. During daytime the sun emits too much light so we can only use this kind of detector during dark,

moonless nights and that is why it only runs about 10% of the time. In the Pierre Auger observatorium there are 24 of these detectors distributed over 4 buildings.[5]

Together these fluorescence and surface detectors form a hybrid detector. When we measure an EAS with the surface detector and at the same time with a fluorescence detector we get complementary information and more accurate measurements than if we only measured this EAS with one of the two detectors. We calibrate the surface detector for the energy with help from the fluorescence detectors. For more information see [5]. This gives us information about the direction, energy and composition of the primary particle.

(a) (b)

Figure 1.3: Here you see the two kinds of detectors a) surface detector [6] b) fluorescence detector [7].

1.4 Radio detectors

If charged particles are influenced by a magnetic field they are bend due to the Lorentz force F_L,

$$\overrightarrow{F_L} = q\overrightarrow{v} \times \overrightarrow{B}. \tag{1.1}$$

In which q is the charge of the particle, $\overrightarrow{v}$ is the speed of the particle and $\overrightarrow{B}$ is the magnetic field. This curvation wil cause the charged particles to emit photons. A result of this Lorentz force is a charge separation: negative and positive charged particles are bent in the opposite direction. This charge separation is another reason that the EAS emits photons. For more information see [8]. We can measure these photons (electromagnetic radiation) with a radio detector.

A radio detector consists of two radio-antenna's one measuring the component of the electromagnetic field in the north-south direction and the the other one in the east-west direction (fig 1.4). We measure the electromagnetic field between 30 and 80 MHz because of the high background noise outside this frequency domain. There are 22 of these detectors installed at the Pierre Auger observatorium. They form the first stage of the Auger Engeneering Radio Array (AERA). An overview of AERA is shown in figure 1.5.

Because the radio detectors are located between the surface and fluorescence detectors we speak of a super-hybrid detector. A super-hybrid event occurs when we measure the same EAS with all the three different techniques. This will increase the precision of the measurements because each technique provides complementary information. A radio detector has a much higher duty cycle than a fluorescence detector.

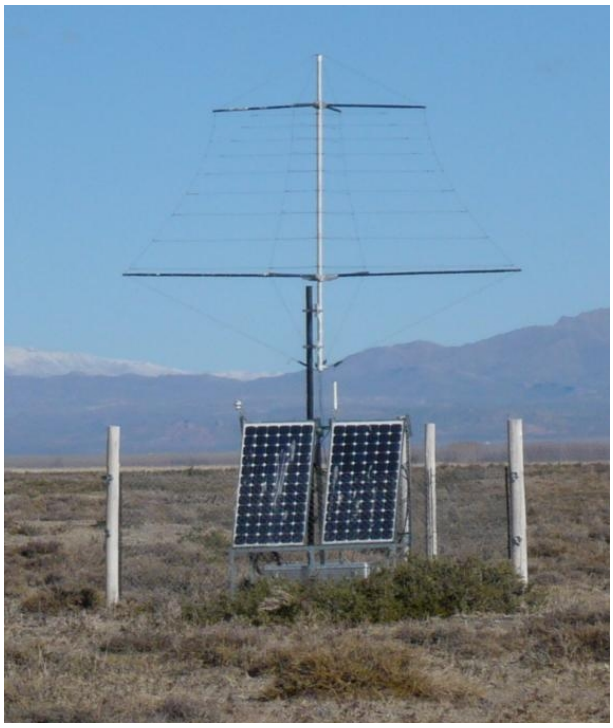

Figure 1.4: A radio detector, it consists of two antenna's measuring the east-west and north-south direction of the electromagnetic field, a solarpanel en behind the solarpanel all kinds of electronics. [9]

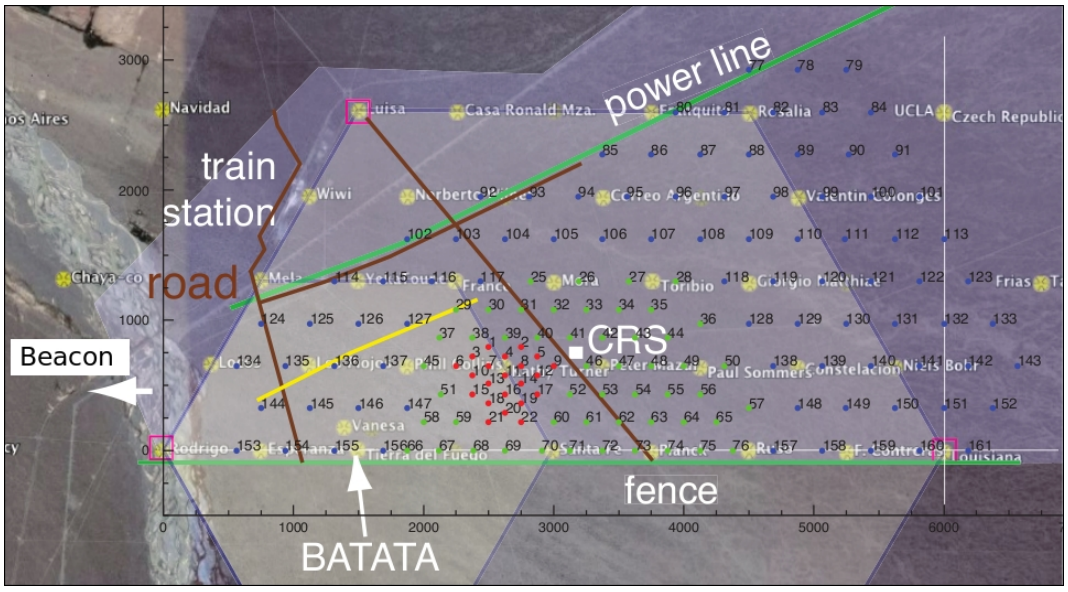

Figure 1.5: A map of AERA, the red points show the locations of the already installed radio detectors. The yellow points show the locations of the surface detectors. The green and blue points show the locations of radio detectors that are planned to be built in the near future. [10]

1.5 Measurements with a radio detector

If we measure an EAS with a radio detector two components of the electromagnetic field are measured. The EAS is not the only source of electromagnetic fields but also all kinds of background sources such as galactic noise, narrowband transmitters and other Radio-Frequency Interference transmitters (RFI's) are present. So there is noise in our measured signal, this noise makes our measurements on an EAS less accurate.

The radio detector itself has an influence on the measurements of EAS's. The detector consist of different parts such as an antenna, an amplifier and other electronics. Therefore, the recorded signal is not the real signal of the EAS but only reflects this signal. Futhermore the time of a measurement is determined by the use of a gps signal (the seconds) and an internal clock in the radio detector for the measurement of the nanoseconds. This clock resets itself every second. There is an a uncertainty in these time measurements . A lot of factors are involved as to the precision of the measurement on an EAS, that is why we want to calibrate the radio detector to correct for these influences.

The measurements performed by a radio detector are saved in the form of a time-series, this time series contains the information of the electromagnetic field in a certain time interval. We can convert this time-series into a frequency spectrum by applying a Fourrier transform, which we need in our analysis.

1.6 The beacon

The gaol of my research is to use the sinuslike transmitted signals from the beacon to calibrate the timing and the gain of the radio detectors and make measurements on EAS's more reliable. In particular the precision of the direction and energy estimates will improve by better timing and gain information.

The beacon is a radio-antenna that is located at a distance of 5.67 km and 174 degrees (from the East) from AERA, detector 11 (see fig. 1.5) and is transmitting continuous sinuslike signals at four different frequencies. The four frequencies are [11]:

$f_1 = 37.793$ MHz,
$f_2 = 46.582$ MHz,
$f_3 = 58.887$ MHz,
$f_4 = 71.191$ MHz.

There is another sinuslike signal that is coming from a different direction from a different source, located in the village of Malargue. This transmitter transmits on the following frequency [11]:

$f_5 = 67.2$ MHz.

2 Beacon-analysis

The radio detectors receive a sinuslike signal on five different frequencies. We can use the received phases and amplitudes of each of the measured signals to respectively determine the stability of the time difference between two radio detectors (phase-analysis) and to relativaly calibrate the amplification of the signal the radio detectors receive with respect to each other (the amplitude-analysis).

2.1 Phase-analysis

2.1.1 Arrival direction reconstruction of EAS's

The direction of an EAS is determined from the arrival times of the signal in several radio detectors. A detector that is close to the EAS shall receive the signal from the EAS earlier than a detector further away from the EAS. We can use these arrival times to determine the direction of the primary particle that caused the EAS. Because we want to know the direction of a primary particle as accurately as possible, we want to know how accurate this time measurement is. We can determine this accuracy by doing the phase-analysis. For more information about the arrival direction reconstruction of the EAS see [12].

2.1.2 Introduction of the phase-analysis

We can use the measured phase differences between two radio detectors to determine the stability of the phase difference in time and thereby also the stability of the time measurement. The phase difference between two radio detectors is not suppose to change, after all the distance between two radio detectors does not change, therefore the path lenght difference between the beacon and each of the detectors is constant. If the phase difference does change it can have different reasons. The beacon does not transmit the signals correctly (eg by a change in frequency), the airpressure is not constant, the temperature of the detector can play a role but more importantly it can be that the internal nanosecond clock of the radio detector is not running at a constant frequency. To determine the cause of instable phase differences between two radio detectors we will use multiple radio detectors as reference detectors with respect to all other detectors. In this analysis we can also determine the accuracy of the determination of the time difference between two detectors.

2.1.3 Determination of the phase difference

The phase difference between detectors i and j for a frequency f_z is (in our case z = 1, 2, 3, 4 or 5; see beacon frequencies chapter 1.6)

$$\Delta\phi_z^{ij} = \phi_z^i - \phi_z^j. \tag{2.1}$$

In which ϕ_z^i and ϕ_z^j are respectively the phase of the signal at detector i and j for frequency f_z.

Because the measurements at each detector takes place separately, there is a time difference in the measurement of the time-series at each detector. That is why we need an additional

factor, the phase difference $\delta^{ij}\phi_z$ that arises if detector i measures at time t_z^i and detector j at an other time t_z^j. This difference is very small in the order of 1 ns but can have a big impact on the phase difference at high frequencies.

The phase difference $\delta^{ij}\phi_z$ caused by this is:

$$\delta^{ij}\phi_z = (dt_z^{ij} * f_z) * 2\pi \tag{2.2}$$

with

$$dt_z^{ij} = t_z^i - t_z^j. \tag{2.3}$$

If we assume that a radiowave has an frequency of about 50 Mhz and $dt^{ij} = 1$ ns then we have a phase difference caused by this effect of 0,3 rad. Thus a difference that we certainly must take into account in our calculations.

The total phase difference between two detectors $\Delta\phi_z^{ij}$ is now represented by

$$\Delta\phi_z^{ij} = \phi_z^i - \phi_z^j - \delta^{ij}\phi_z. \tag{2.4}$$

2.1.4 Uncertainty in the phase difference

The phases are determined by making a Fourier transform of the time series, and using the complex information in the frequency space, which then provides phase and amplitude. The measured phase difference between two detectors for a frequency f_z has an uncertainty. We can calculate the maximum error in the determination of the phase difference if we know the maximum uncertainty in the amplitude of the signal S_z, which originates from a noise contribution. We determine the noise in the amplitude of the measured signal by taking the average amplitude of the measured frequency spectrum 1 MHz beneath and 1 MHz above the measured frequency f_z. We call this amplitude N_z (amplitude of the noise). This will give us an estimate of the noise in our frequency bin. The influence of the noise in our measured amplitude is maximal when the noise is in phase with the signal from the beacon or when it is precisly 180 degrees out of phase. The measured amplitude S_z^i at a detector i is then given by

$$S_z^i = R_z^i \pm N_z^i. \tag{2.5}$$

In which R_z^i is the real amplitude from the signal transmitted by the beacon at frequency f_z received at detector i. Therefore R_z^i is given by

$$R_z^i = S_z^i \pm N_z^i. \tag{2.6}$$

And the uncertainty used will be N_z^i. The maximum uncertainty in the phase measurement of detector i is given by

$$\sigma_{\phi_z}^i = arctan(N_z^i/S_z^i) \tag{2.7}$$

as can be understood by looking at the following picture (figure 2.1).

We can now use this to determine the uncertainty in the phase difference between detectors i and j $\sigma_{\Delta\phi_z}^{ij}$ using standard error propagation, assuming the uncertainties at the different stations are uncorrelated, as given by formula 3.1 (appendix 3.1) which results in:

$$\sigma_{\Delta\phi_z}^{ij} = \sqrt{(\sigma_{\phi_z}^i)^2 + (\sigma_{\phi_z}^j)^2} = \sqrt{(arctan(N_z^i/S_z^i))^2 + (arctan(N_z^j/S_z^j))^2}. \tag{2.8}$$

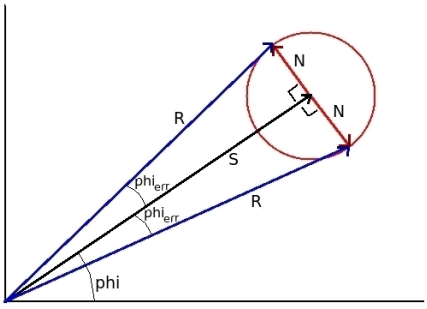

Figure 2.1: The noise has the maximum influence on the phase of R if it is exactly 90 degrees out of phase with S. So the maximum error in the phase is given by $\arctan(N/S)$.

2.1.5 Time stability

We now define a measurement of time stability. For one measurement and a certain frequency f_z we can determine the phase difference between two detectors. The total time T_z^{ij} that a signal from detector i is on its way to detector j for a frequency f_z is given by:

$$T_z^{ij} = \frac{n_z}{f_z} + \frac{\Delta\phi_z^{ij}}{2\pi f_z} \tag{2.9}$$

In which n_z is the wavenumber for frequency f_z and thus only has integer values. We use this formula for the measured phase differences for frequencies f_2, f_3, f_4 and f_5 between two detectors. We do not use frequency f_1 because the signal to noise ratio is too low and for the other frequencies I only used measurements with a signal to noise ratio above 3, see appendix 3.2. For each frequency f_z with z = 1, 2, 3, 4 and 5 T_z^{ij} has to be the same, all electromagnetic signals travel with the speed of light, this gives us the following equation for the travel time of the signal between detector i and j T^{ij}

$$T^{ij} = \frac{n_2}{f_2} + \frac{\Delta\phi_2^{ij}}{2\pi f_2} = \frac{n_3}{f_3} + \frac{\Delta\phi_3^{ij}}{2\pi f_3} = \frac{n_4}{f_4} + \frac{\Delta\phi_4^{ij}}{2\pi f_4} = \frac{n_5}{f_5} + \frac{\Delta\phi_5^{ij}}{2\pi f_5}. \tag{2.10}$$

In which I have used 2, 3, 4 and 5 to denote the according wavenumber and phasedifference for respectively frequency f_2, f_3, f_4 and f_5. We are going to look for which wavenumbers, n_2, n_3, n_4 and n_5, this equation holds.

Unfortunately, in the analysis a complete 2pi phase rotation cannot be determined. Therefore, the integer values n_2, n_3, n_4 and n_5 will not be fixed from the measurement itself. However, we can assume that the time difference T^{ij} has to be small, and use the integer numbers in such a way that the time difference as determined by each of the frequencies will be the same within the uncertainties. See figure 2.2 for clarification.

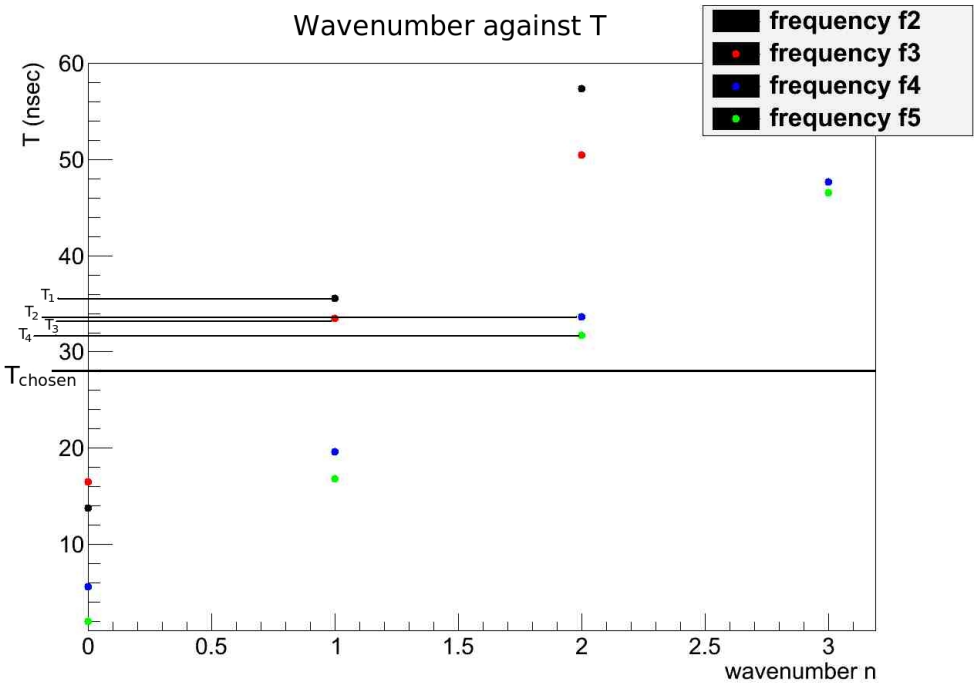

Figure 2.2: Formula 2.5 plotted in a graph for different frequencies, for a certain measurement of the phase difference between detector 1 and 11 ($\Delta\phi^{1,11}$). T_1, T_2, T_3 and T_4 are respectively the $T_z^{1,11}$ for frequency f_2, f_3, f_4 and f_5. So $T_z^{1,11}$ depends on $T^{1,11}$ and the frequency.

We now have to look for those wavenumbers n_2, n_3, n_4 and n_5, and respectively T_2^{ij}, T_3^{ij}, T_4^{ij} and T_5^{ij} and T^{ij} for which $T^{ij} = T_2^{ij} = T_3^{ij} = T_4^{ij} = T_5^{ij}$ this will be the according time for which formula 2.10 holds. When the obtained time differences are exactly the same for each frequency the real result is obtained. However, due to measurement uncertainties this is unlikely to happen. therefore I created a measure for the goodness of a specific time difference measurement as follows:

$$R^{ij} = (T^{ij} - T_2^{ij})^2 + (T^{ij} - T_3^{ij})^2 + (T^{ij} - T_4^{ij})^2 + (T^{ij} - T_5^{ij})^2. \tag{2.11}$$

In which we call R^{ij} the residue. If the residue is zero than formula 2.10 holds. We have to take into account that $(T^{ij} - T_z^{ij})$ has an uncertainty. We are going to weigh each $(T^{ij} - T_z^{ij})$ with its uncertainty $\sigma_{T_z}^{ij}$ which arises due to the uncertainty in the phase measurement $\sigma_{\phi_z}^{i}$ and $\sigma_{\phi_z}^{j}$. Then formula 2.11 becomes:

$$R^{ij} = (\frac{T^{ij} - T_2^{ij}}{\sigma_{T_2}^{ij}})^2 + (\frac{T^{ij} - T_3^{ij}}{\sigma_{T_3}^{ij}})^2 + (\frac{T^{ij} - T_4^{ij}}{\sigma_{T_4}^{ij}})^2 + (\frac{T^{ij} - T_5^{ij}}{\sigma_{T_5}^{ij}})^2. \tag{2.12}$$

where $\sigma_{T_z}^{ij}$ is determined with formula 3.1:

$$\sigma_{T_z}^{ij} = \sqrt{(\frac{\sigma_\phi^i}{2\pi f_z})^2 + (\frac{\sigma_\phi^j}{2\pi f_z})^2}. \tag{2.13}$$

In which z can be again 2, 3, 4 and 5.
We want to minimize the residue, so search for which T^{ij} the residue has the lowest value. In figure 2.3 a graph is shown of the residue for a measurement between detector 6 and 7. $T^{6,7}$ is chosen between 0 and 150 ns. You can clearly see that the residue almost is zero for a couple of points but it never reaches zero this is due to the uncertainty in the time measurement and the phase difference.

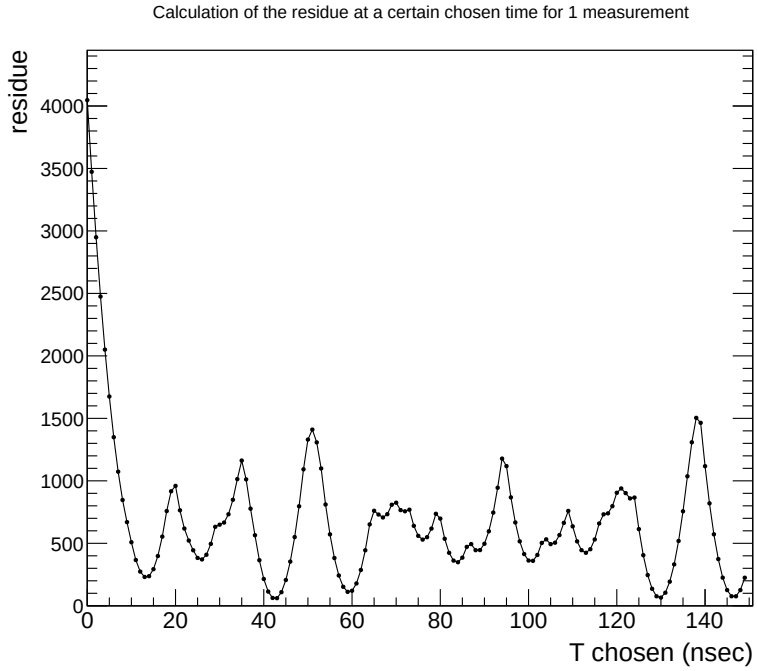

Figure 2.3: The calculated residue against $T^{6,7}$ of one measurement of the phase difference between radio detector 6 and 7. You can see that there are a couple of points where the residue almost is zero.

We are going to do this analysis not for one measurement of the phase difference between two detectors but for a lot of measurements, this tells us something about the development of the minima of the residue over time. I looked at data for 6 days (see appendix 3.3), during which a measurement is made every 10 seconds. In figure 2.4 the determination of the residue between detectors 1 and 4 over a period of 6 days is displayed.

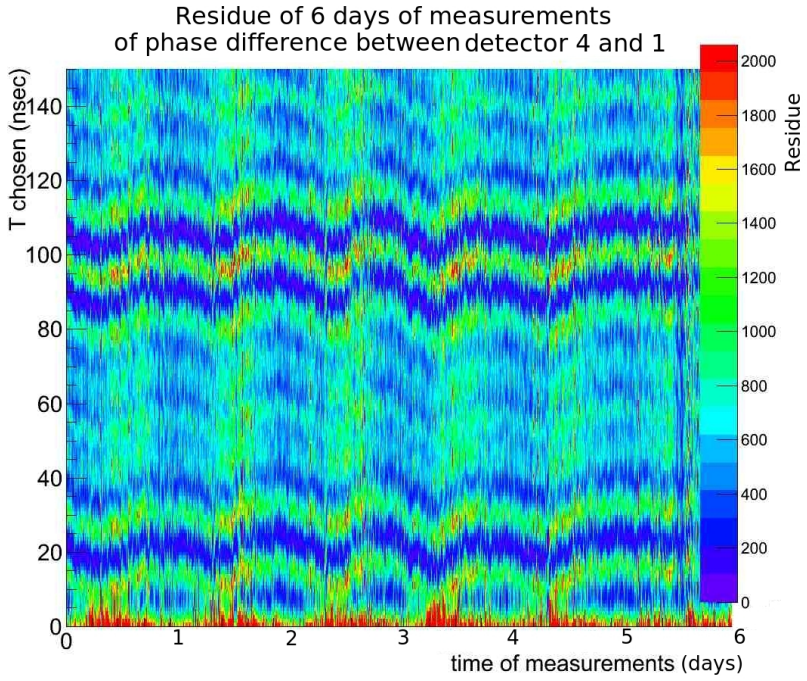

Figure 2.4: A graph of the residue over 6 days. You can see that there are several minima of the residue and that those minima change in time.

Figure 2.4 shows that the minima of the residue change over time and that there are several minima, so we cannot say anything about the real time a signal is on its way from one detector to an other one. But what we can do is determine the stability of a time measurement between two stations.

Now I am going to look at a random minimum residue in figure 2.4 and determine how much this changes in time. I can take a random minima because all the minima you see in figure 2.4 change in the same way over time. I have done this using detector 4 as a reference detector and display the timing of the minimum residue between this detector and all the other detectors in figure 2.5.

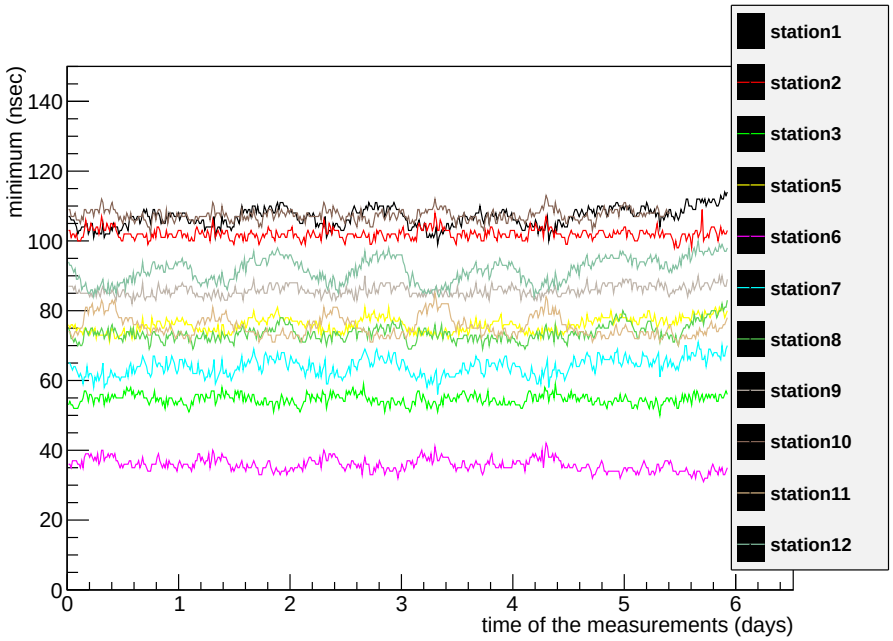

Figure 2.5: The development of the timing of the minima of the residue for the different detectors using detector 4 as reference detector.

To say somethinig about the stability of the time measurement we want to make sure we have a reference detector that is stable (so it does not depend on the detector that the phase difference and thus the residue changes over time). That is why I am going to take all the detectors as reference detector once. I then compare the results and determine for which reference detector the minima of the residue change the least in time. The graphs of the minima of the other detectors as reference detector are shown in figures 2.6 and 2.7. It appears that detector 4 provides the most stable results.

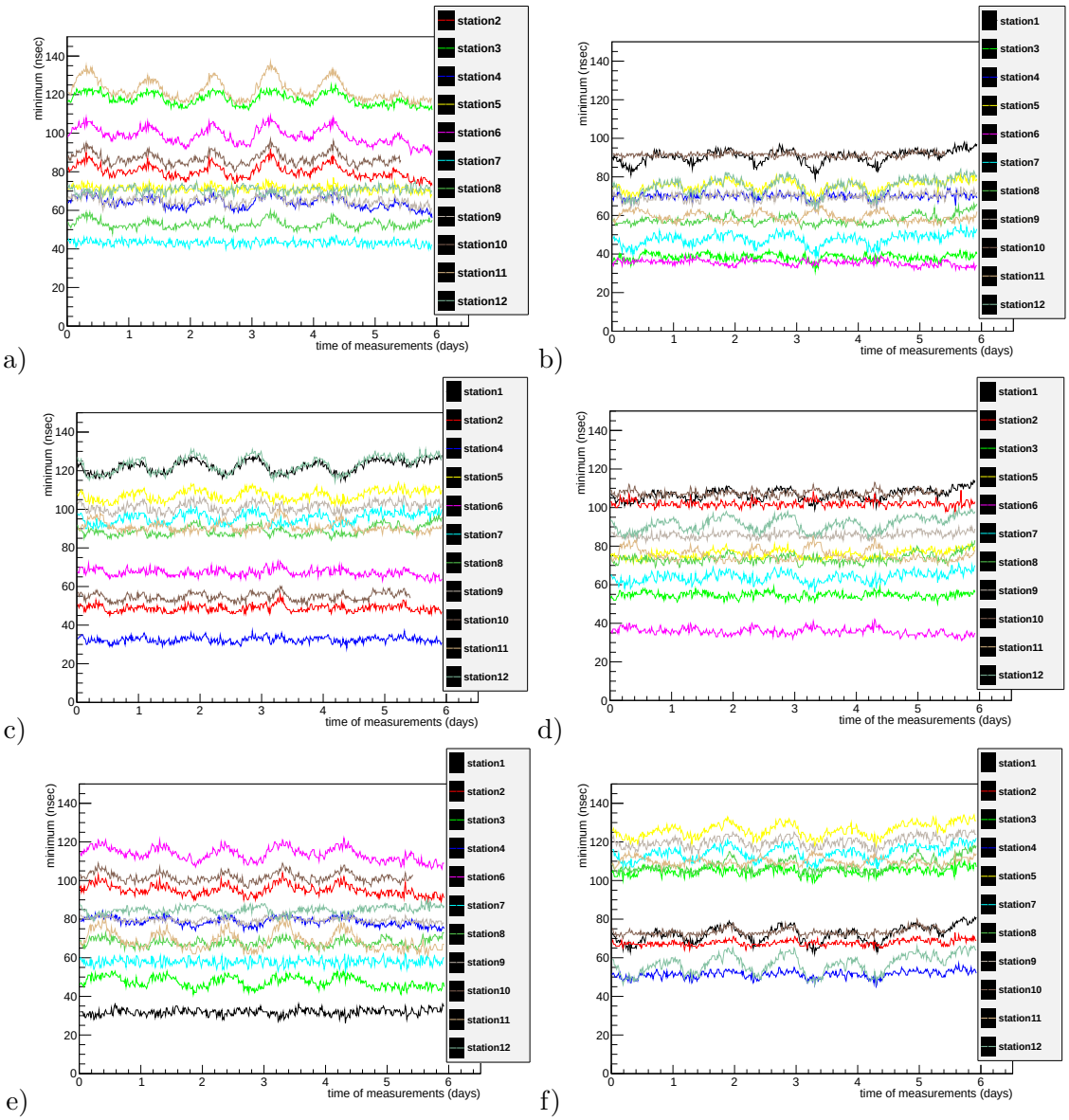

Figure 2.6: Development of minima in time of different reference detectors with respect to the other detectors (a) ref.station 1, (b) ref.station 2, (c) ref.station 3, (d) ref.station 4, (e) ref.station 5, (f) ref.station 6.

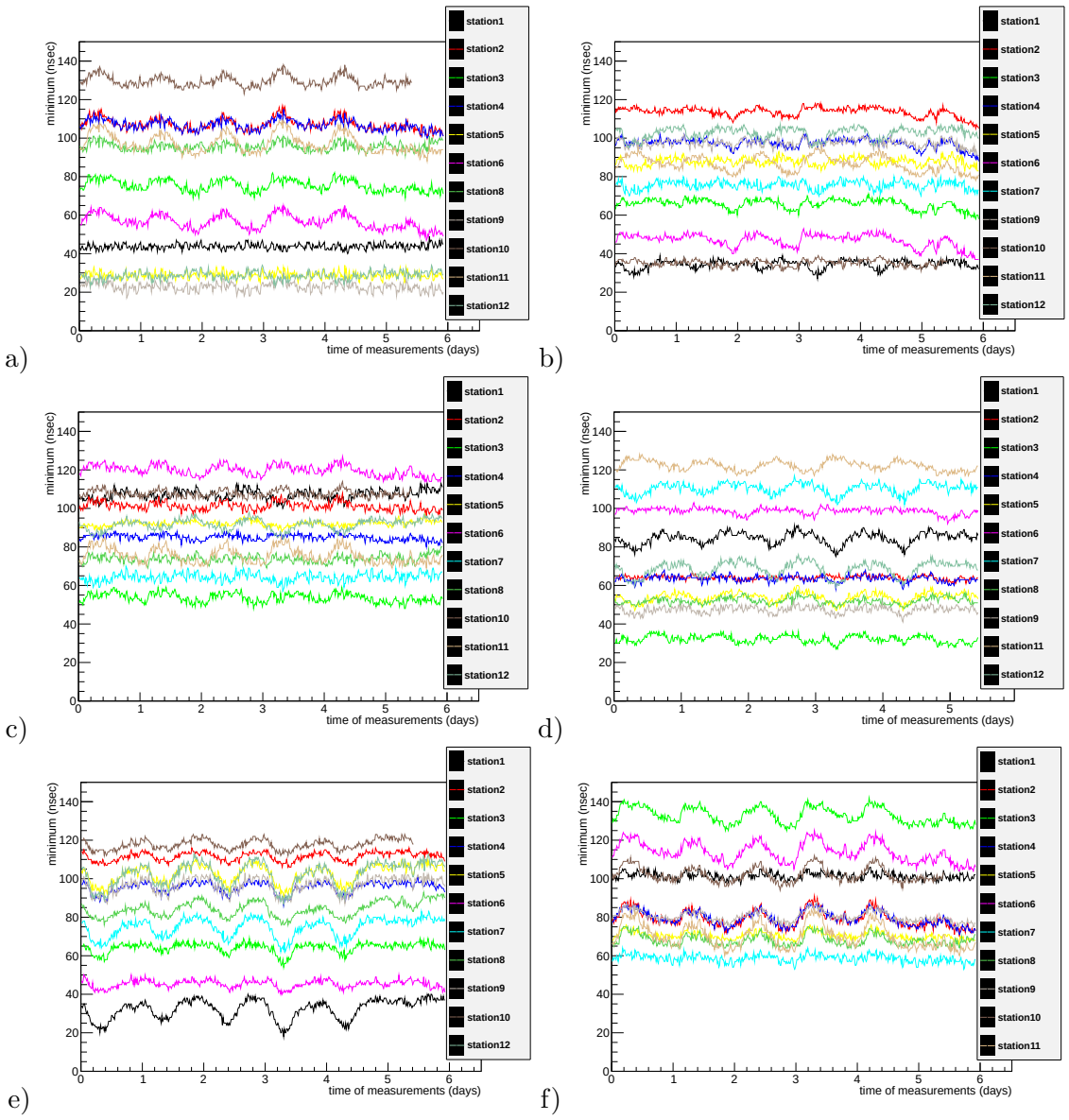

Figure 2.7: Development of minima in time of different reference detectors with respect to the other detectors (a) ref.station 7, (b) ref.station 8, (c) ref.station 9, (d) ref.station 10, (e) ref.station 11, (f) ref.station 12.

By looking at the change in the minima of the residue over time the source of this change can be determined. This source can either be an external factor or an internal factor (detector dependend). When all the minima of the residue change the same for each pair of detectors in time it is more likely that a external factor is the cause other wise it might be a internal factor. In figures 2.6 and 2.7 you clearly see a oscillation in the minima of the residue in time. It looks like the day and night cycle has something to do with it which indicates that external factors play a role. The beacon can transmit differently during night or day time. The temperature and airpressure can have an effect on the propagation of the signal through the air (change in refractive index of air during night and day time [13]). On some detectors this oscillation is almost gone this can have different reasons, the detectors have opposite oscillation in the measurement of the phase of the signal or the detectors do not have an oscillation in the phase measurement at all.

Using detector 4 as a reference from now on, I am going to look at the spread of the minima of the residue over time. This spread tells us how stable the time measurement between two detectors is. I fitted the spread of the minima of the timing of the residue with a gaussian. See the results in figures 2.8 and 2.9. You can see that a gaussian is not always a proper description of the spread but nevertheless we can use the sigma as a measure of the stability of the time measure. The sigma values vary between 2,4 and 4,1 ns. Note that secondary bumps can appear when moving from one minimum series to another (see figure 2.4). When assuming that station 4 has a timing precision of 2.4/sqrt(2)=1.7 ns, the precision of the other stations varies between 1.7 and 3.7 ns.

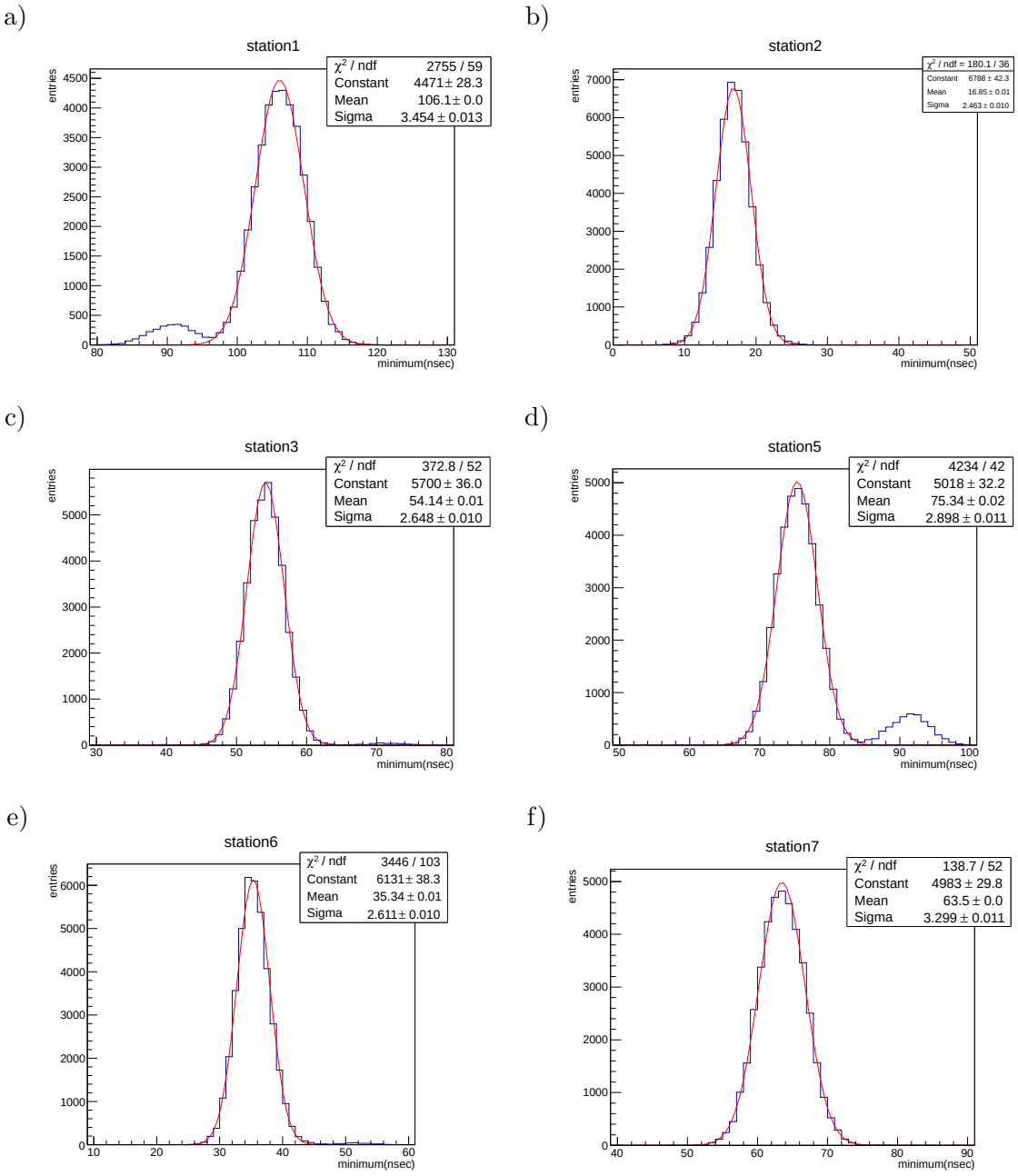

Figure 2.8: Spread of a minimum of the residue with detector 4 as reference detector and the other detectors: (a) detector 1, (b) detector 2, (c) detector 3, (d) detector 5, (e) detector 6, (f) detector 7.

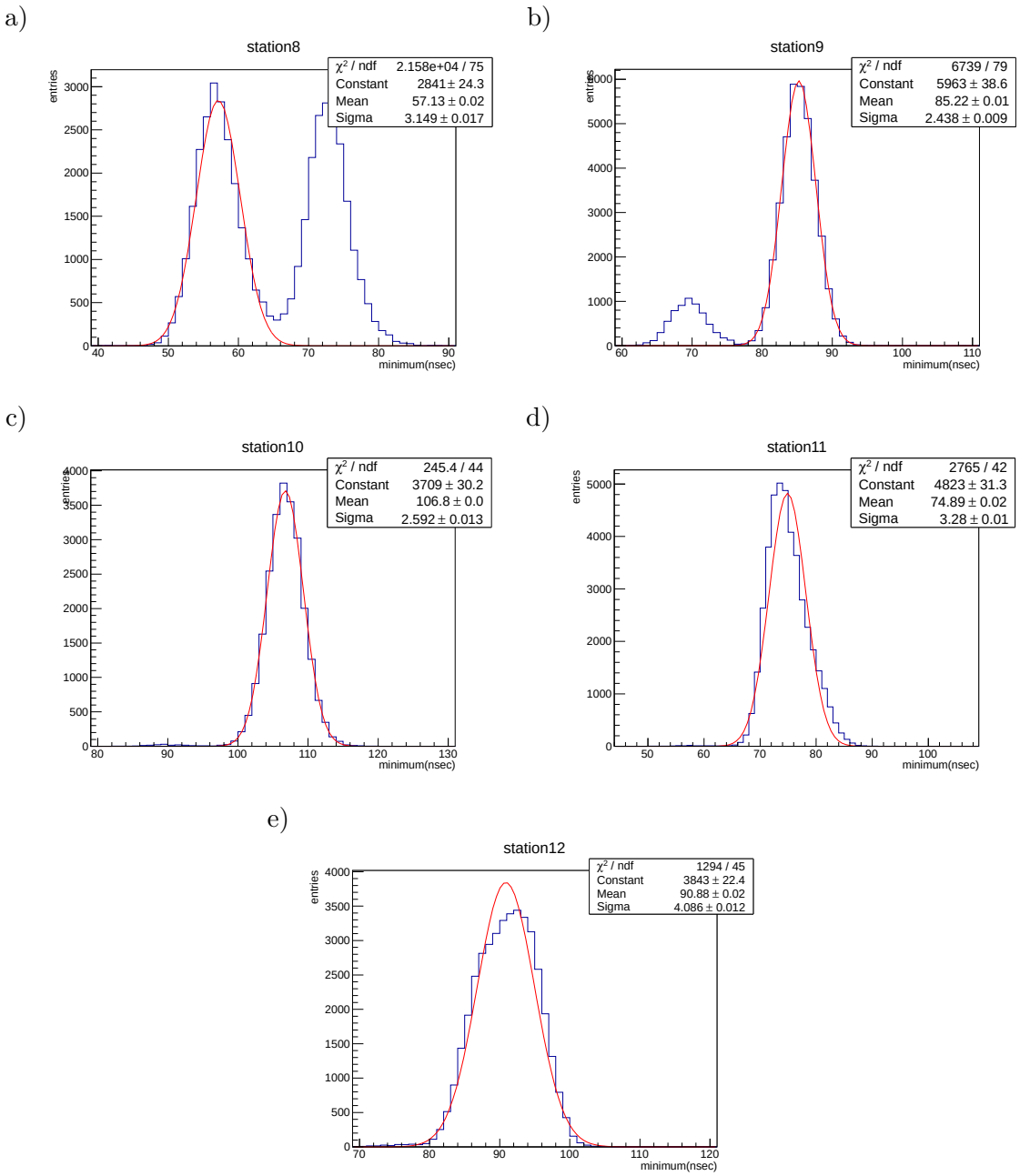

Figure 2.9: Spread of a minimum of the residue with detector 4 as reference detector and the other detectors: (a) detector 8, (b) detector 9, (c) detector 10, (d) detector 11 (e) detector 12.

2.2 Amplitude-analysis

2.2.1 Energy reconstruction of EAS's

The energy of an EAS can be measured with a fluorescence detector and a surface detector. We can calibrate a radio detector for the energy if we measure an EAS simultaneously with a a radio detector and a fluorescence detector or a surface detector. I will explain in short how we do this. For each measurement of an EAS by the radio detectors we can determine a signal strenght S_0 at a certain distance D_0 from the showercore (see figure 2.10a). We can do this for different measurements of the signal strenght S of different EAS's and determine for each EAS the value of S_0 the only requirement is that these EAS's are also measured by a fluorescence or a surface detector. Now we can use the measured S_0 and the measured energy of the EAS by the fluorescence or surface detector to determine the energy of the EAS with a radio detector. See figure 2.10b.[14]

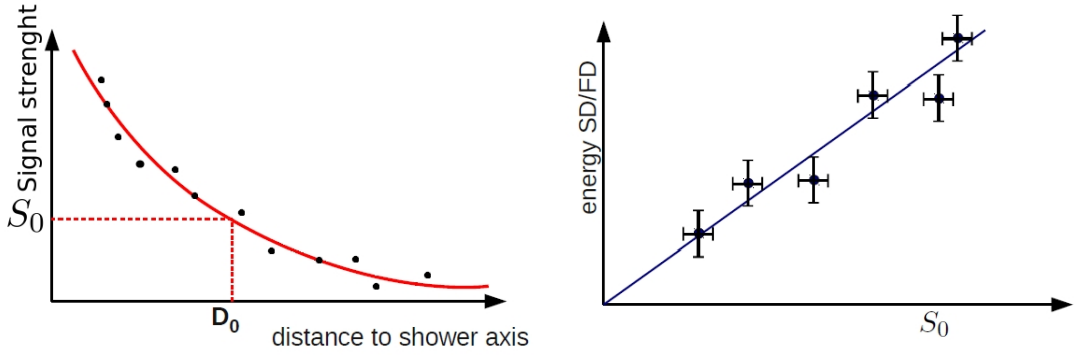

(a) (b)

Figure 2.10: a) Determine the signal strenght at a distance D_0 from the shower axis for the radio detectors. b) Energy calibration with the other detection methods.

It is important to determine the signal strenght at a distance D_0 as good as possible. That is why we have to calibrate the radio detectors for the amplification of the measured signal strenght with respect to each other. If one detector amplifies the incoming signal more than an other detector we do not get a good value for S_0.

2.2.2 Introduction to the amplitude-analysis

The beacon is located at 5.67 km and 174 degrees of detector 11 (see figure 1.5) and we know the location of our detectors to an accuracy of 10 cm. So we plot the measured amplitude per detector per frequency against the distance from the beacon to that detector. If we do this we can adjust the amplification of the measured signal in each detector to the correct amplitude value with respect to the other detectors.

2.2.3 Amplitude calibration

We are going to measure the amplitude during 6 days (data set used, defined in appendix 3.3) for each frequency of the beacon (except frequency f_1 because of the low signal to noise ratio and only use measurements for the other frequencies of the beacon with a signal to noise ratio above 3, see appendix 3.2) as measured by each detector. First I am going to look at the amplitude variations in time for these 6 days. Figure 2.11 shows the amplitude as a function of time for frequency f_2 as measured by detector 1. For all the other amplitudes of all the frequencies and detectors see appendix 3.4. You can clearly see in figure 2.11 a day and night cycle in the amplitude but the maximum and minimum values remain the same during this period. In figures 3.14 - 3.18 this is not always the case. During the measurement of this data set (appendix 3.3) some of detectors were not working correctly, a couple detectors had broken antenna wires. This

can be a possible explanation for the differences measured by some detectors for the amplitude as a function of time.

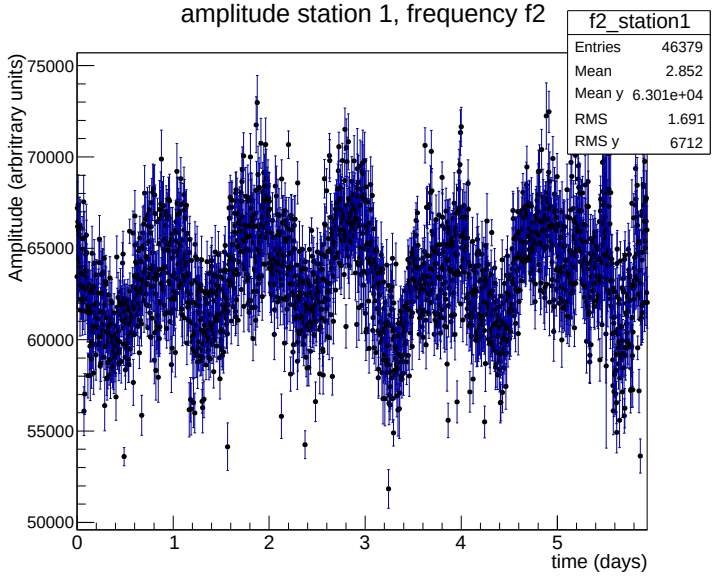

Figure 2.11: Measured amplitude displayed versus the time for frequency f_2 and detector 1.

We can also determine the spread of the amplitude during these 6 days for a certain frequency and for a detector. I fitted a gaussian to this spread, we can use the mean of the gaussian fit as a measure of the amplitude and de sigma value as the uncertainty in the amplitude, see figure 2.12.

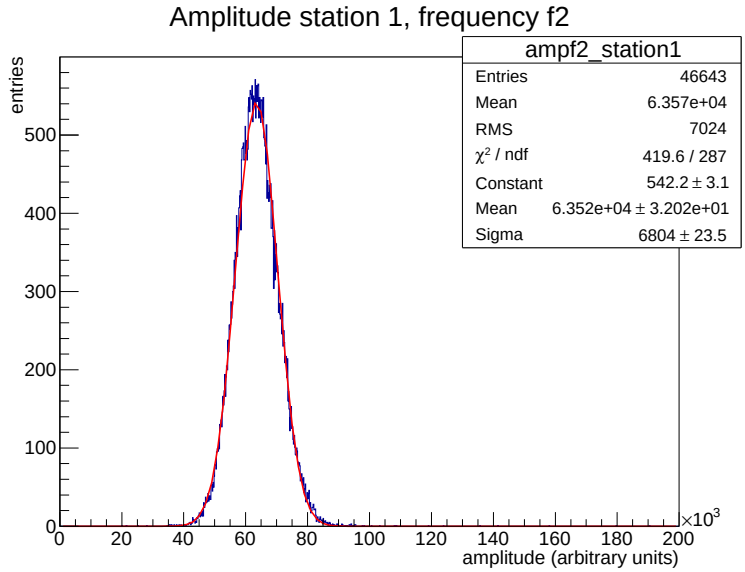

Figure 2.12: Measured amplitude for frequency f_2 for detector 1. A gaussian function is fitted, the mean gives us a measure of the amplitude.

I have determined the amplitudes and their uncertainties for all detectors and all frequencies (see appendix 3.5) and in the figures 2.11, 2.12 and 2.13 I have plotted these amplitudes against the distance from the detector to the beacon per frequency. Because the expected intensity of the signal from the beacon is proportional to the inverse square law:

$$intensity \propto \frac{1}{distance^2} \tag{2.14}$$

I fitted the following function to the data points

$$P = \frac{p_0}{x^2} + p_1. \tag{2.15}$$

In which p_0 is the fitparameter which defines the intensity of the electromagnetic signal at the beacon, p_1 gives us the noise in the signal and x is the distance from the beacon for a detector.

If the amplifaction of the signal at the three frequencies is detector independend you expect to see the same relative amplitude between the detectors for each frequency. You can see that in all the figures amplitude of the signal at detector 11 lays far above the fitted function. This indicates that detector 11 has a higher signal amplification. The relative amplitude at detector 10 varies for different frequencies. This is probably due to the fact that a wire of detector 10 was broken and it was less sensitive to frequency f_3 than for the other frequencies. You can also see that detector 12 is much less sensitive for frequency f_4 than for the other frequencies probably due to the same effect. See appendix 3.6 for a report of the broken wires.

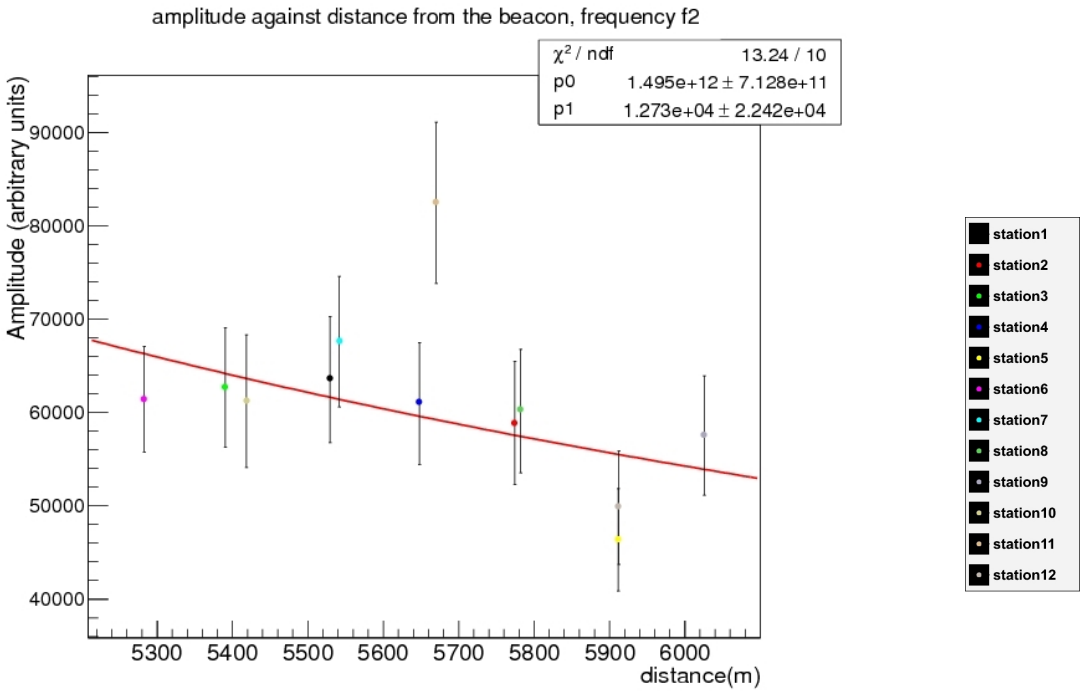

Figure 2.13: The measured amplitude per detector displayed against the distance from the beacon for frequency f2. The red line indicates the fitted function P with p_0 and p_1 its fitparameters.

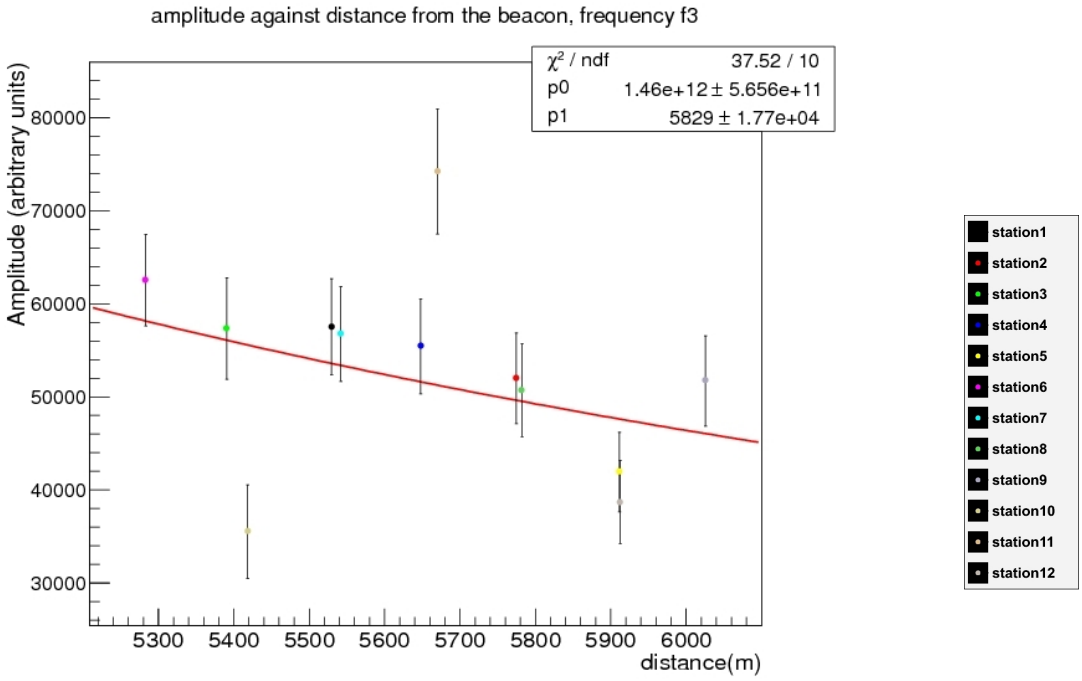

Figure 2.14: The measured amplitude per detector displayed against the distance from the beacon for frequency f3. The red line indicates the fitted function P with p_0 and p_1 its fitparameters.

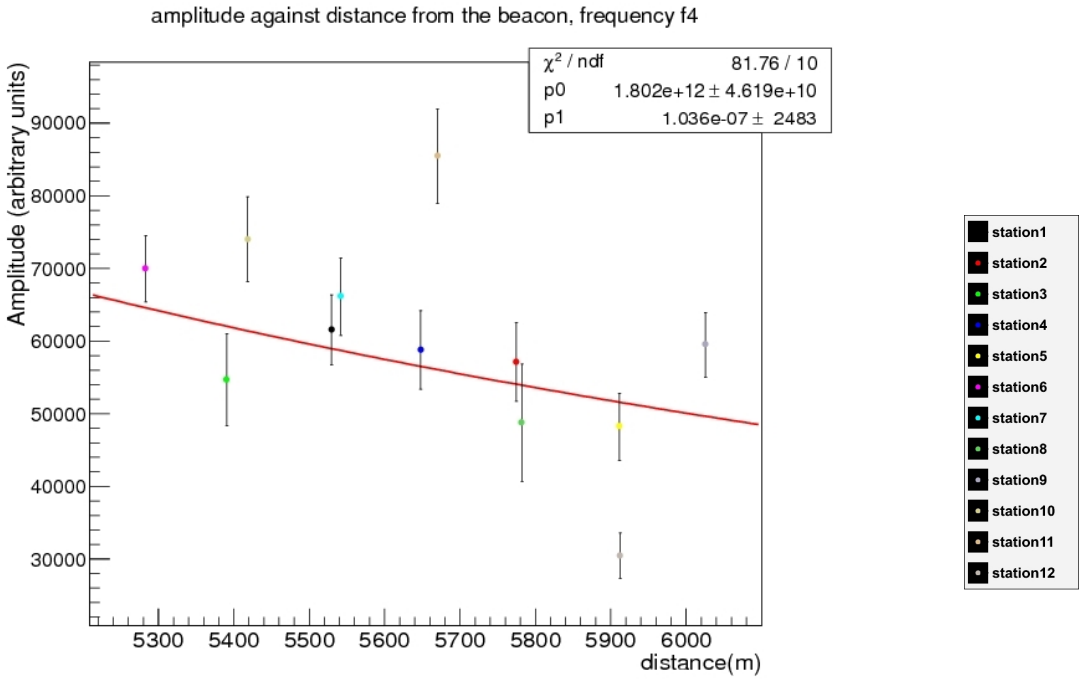

Figure 2.15: The measured amplitude per detector displayed against the distance from the beacon for frequency f4. The red line indicates the fitted function P with p_0 and p_1 its fitparameters.

Because of the broken wires the relative amplitude calibration of the detectors to each other for the amplification of the amplitude of a measured signal is not very accurate, and the fitparameters are not determined very well. We can determine the factor for which we have to

correct the amplification of the amplitude of a measured signal at each detector. See table 1.

table 1: factor correction for frequency f_2, f_3 and f_4

Detector	factor f_2	factor f_3	factor f_4
1	1.03	0.93	0.96
2	1.02	0.95	0.95
3	0.98	0.98	1.13
4	1.02	0.93	0.96
5	1.20	1.14	1.07
6	1.08	0.93	0.92
7	0.91	0.94	0.89
8	0.96	0.98	1.11
9	0.94	0.89	0.83
10	1.04	1.57	0.82
11	0.72	0.69	0.66
12	1.12	1.23	1.69

2.3 Conclusion and discussion

The phase-analysis gives us an estimate of the stability of the time measurement between two detectors. The stability of the time measurement between two detectors is in the order of a couple of ns. An other study is needed to determine if we indeed can use this uncertainty in the time measurement to correct for this influence in the direction reconstruction of EAS's. We see an oscillation in the minima of the residue in time. It appears an external factor is the main cause because of the oscillation during day and night. However, this does not explain why some pairs of detectors have not got an oscillation at all. Probably a measurement of the minima of the residue for a longer period is needed.

The amplitude-analysis shows that detector 11 has a larger amplification. For the other detectors we cannot say very much beacuse of the uncertainty in the amplitude of the measured signal at the detectors due to the broken wires. Another data set has to be analyzed and the distance to the beacon has to be determined more accuratly. But nevertheless this gives us a good indication of the relative amplification of each detector with respect to the other detectors.

Bibliography

[1] A.A.Watson, "Cosmic rays of the highest energies", Contemporary Physics,2002, volume 43, number 3, pages 181-195

[2] http://www.expeditions.udel.edu/antarctica08/blog-dec-12-2008.html

[3] http://www.augeraccess.net/Pierre_Auger_Observatory.htm

[4] J. Abraham et al. [Pierre Auger colabiration],"Trigger and aperture of the surface detector array of the Pierre Auger Observatory", 2012

[5] J. Abraham et al. [Pierre Auger colabiration], "The fluorescence detector of the Pierre Auger Observatory", 2010

[6] http://physicschool.web.cern.ch/PhysicSchool/LatAmSchool/2005/

[7] http://www.auger.org/observatory/pics/FDs_sm.jpg

[8] Harm Schoorlemmer, "Tunning in on cosmic rays", ISBN: 978-90-9027039-5, chapter 2

[9] picture out of the bachelor thesis from Katherina Holland, "The influence of noise on radio signals from cosmic rays", page 8

[10] https://www.auger.unam.mx/AugerWiki/AERA%2C_systems_integration%2C_deployment

[11] Frank Gerhard Schröder, thesis: "Instruments and Methods for the Radio Detection of High Energy Cosmic Rays", december 2010, chapter 5

[12] José Coppens, "Cosmic rays are on the air", 2011, ISBN: 978-90-9026370-0, chapter 6, page 87

[13] James C.Owens, "Optical Refractive Index of Air: Dependence on Pressure, Temperature and Composition", January 1967

[14] Christian Glaser, private communication.

3 Appendix

3.1 Propagation of error

Given $X = f(A, B, C, ..)$

$$\sigma_X^2 = (\frac{\delta f}{\delta A}\sigma_A)^2 + (\frac{\delta f}{\delta B}\sigma_B)^2 + (\frac{\delta f}{\delta C}\sigma_C)^2 + ... \tag{3.1}$$

3.2 Signal to Noise ratio

The signal to noise ratio is the ratio of the amplitude of the measured signal S and the amplitude of the noise N in that signal:

$$\frac{S}{N} \tag{3.2}$$

The spread in the signal to noise ratio's for all frequencies and detectors are shown in the following figures.

frequency f_1

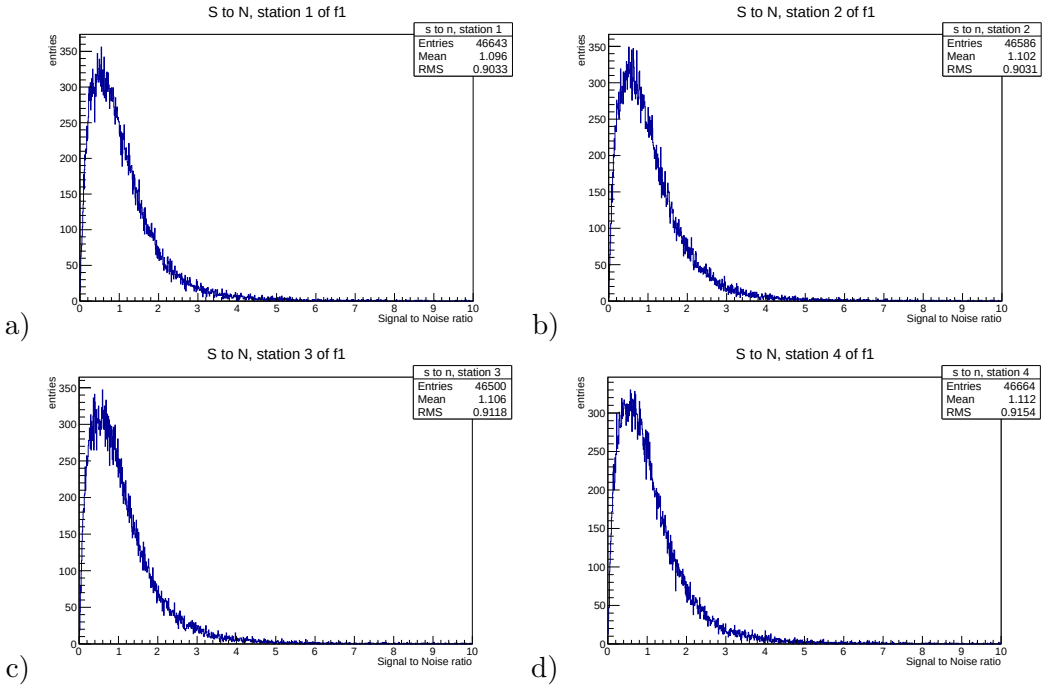

Figure 3.1: Signal to noise ratio S/N for frequency f1 for (a) detector 1, (b) detector 2, (c) detector 3, (d) detector 4.

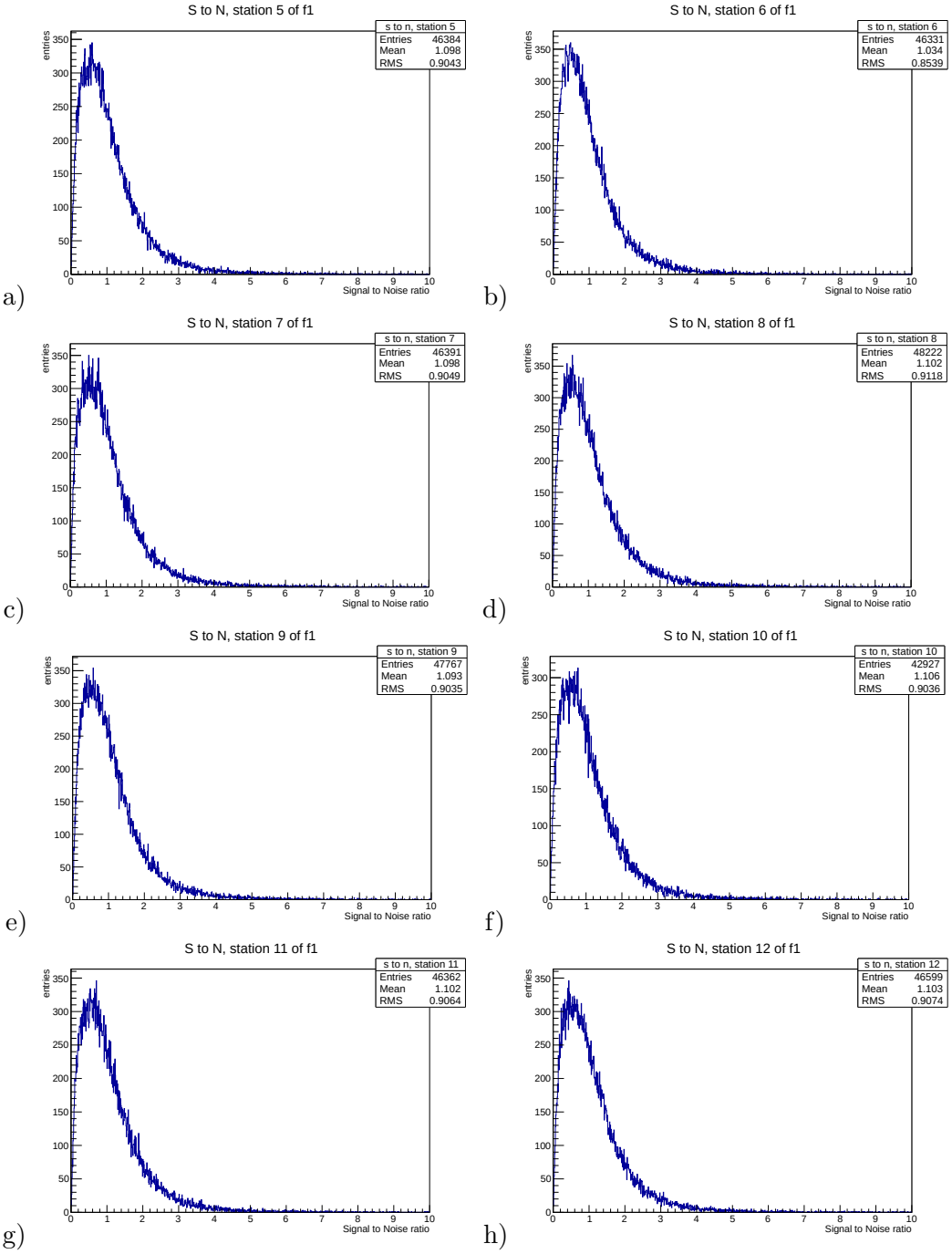

Figure 3.2: Signal to noise ratio S/N for frequency f1 for (a) detector 5, (b) detector 6, (c) detector 7, (d) detector 8, (e) detector 9, (f) detector 10, (g) detector 11, (h) detector 12.

frequency f_2

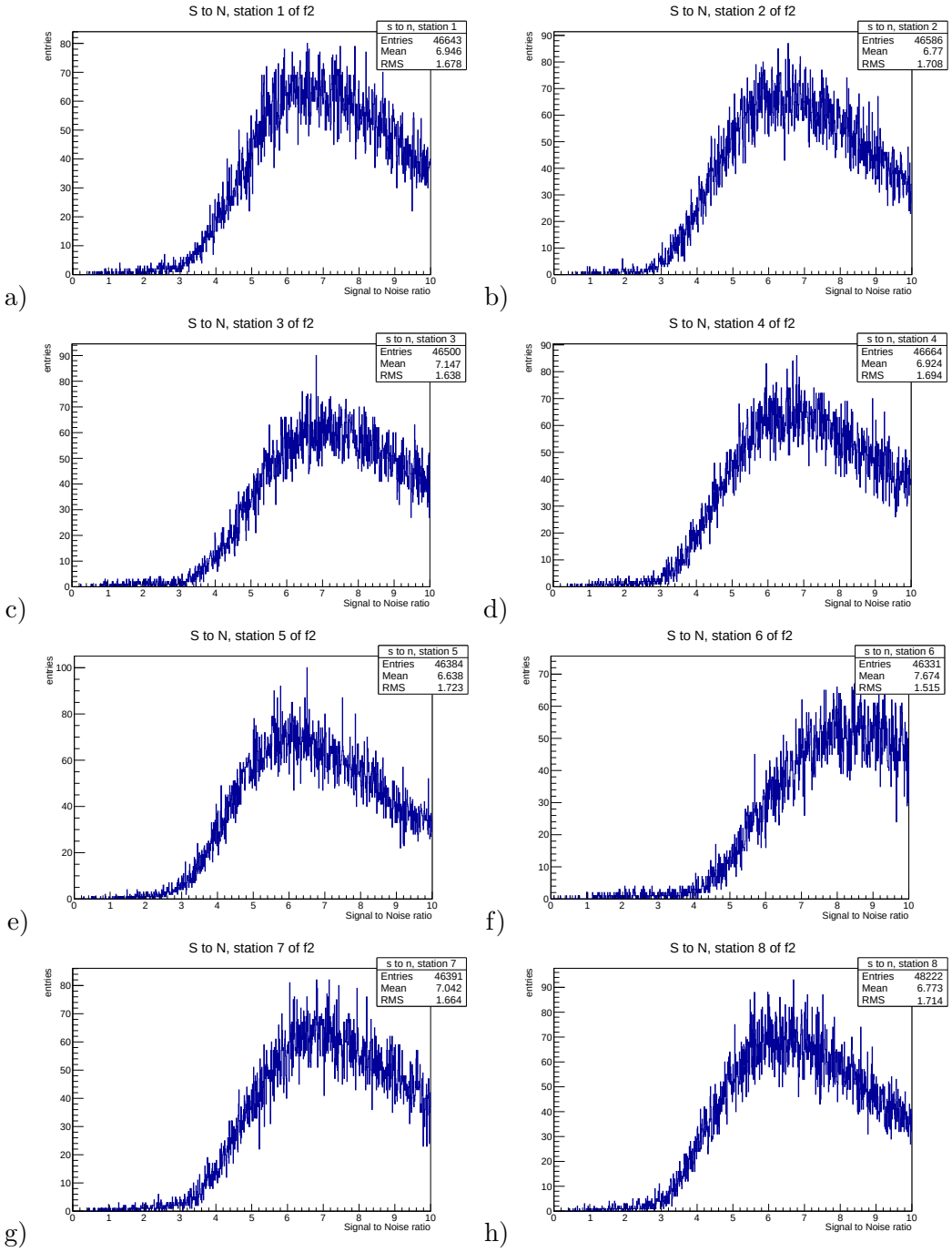

Figure 3.3: Signal to noise ratio S/N for frequency f2 for (a) detector 1, (b) detector 2, (c) detector 3, (d) detector 4, (e) detector 5, (f) detector 6, (g) detector 7, (h) detector 8.

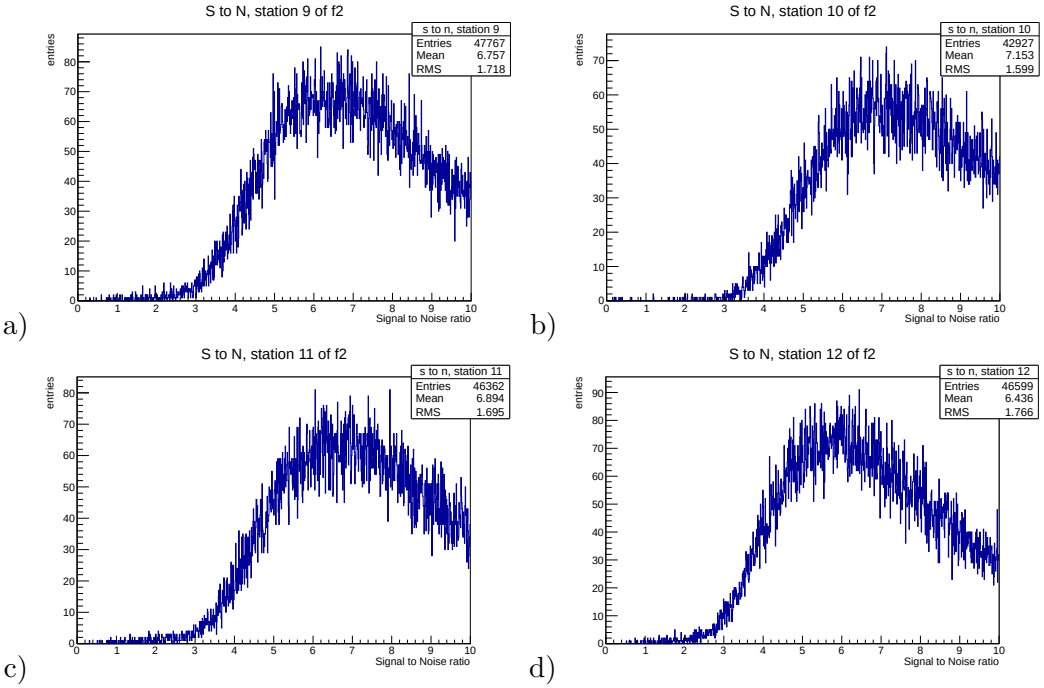

Figure 3.4: Signal to noise ratio S/N for frequency f2 for (a) detector 9, (b) detector 10, (c) detector 11, (d) detector 12.

frequency f_3

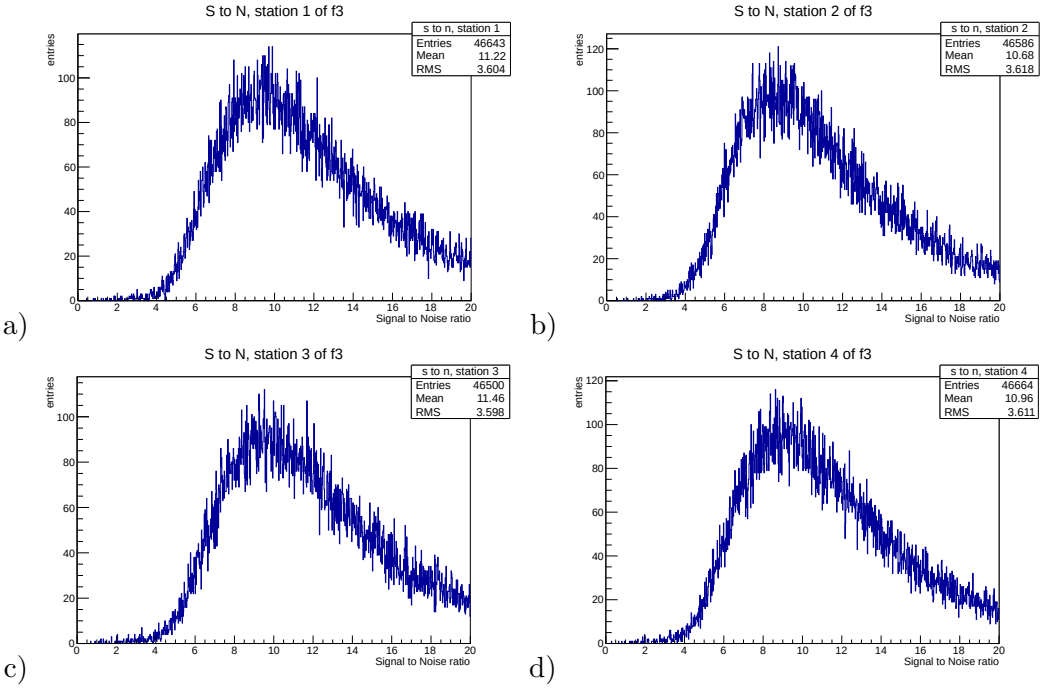

Figure 3.5: Signal to noise ratio S/N for frequency f3 for (a) detector 1, (b) detector 2, (c) detector 3, (d) detector 4.

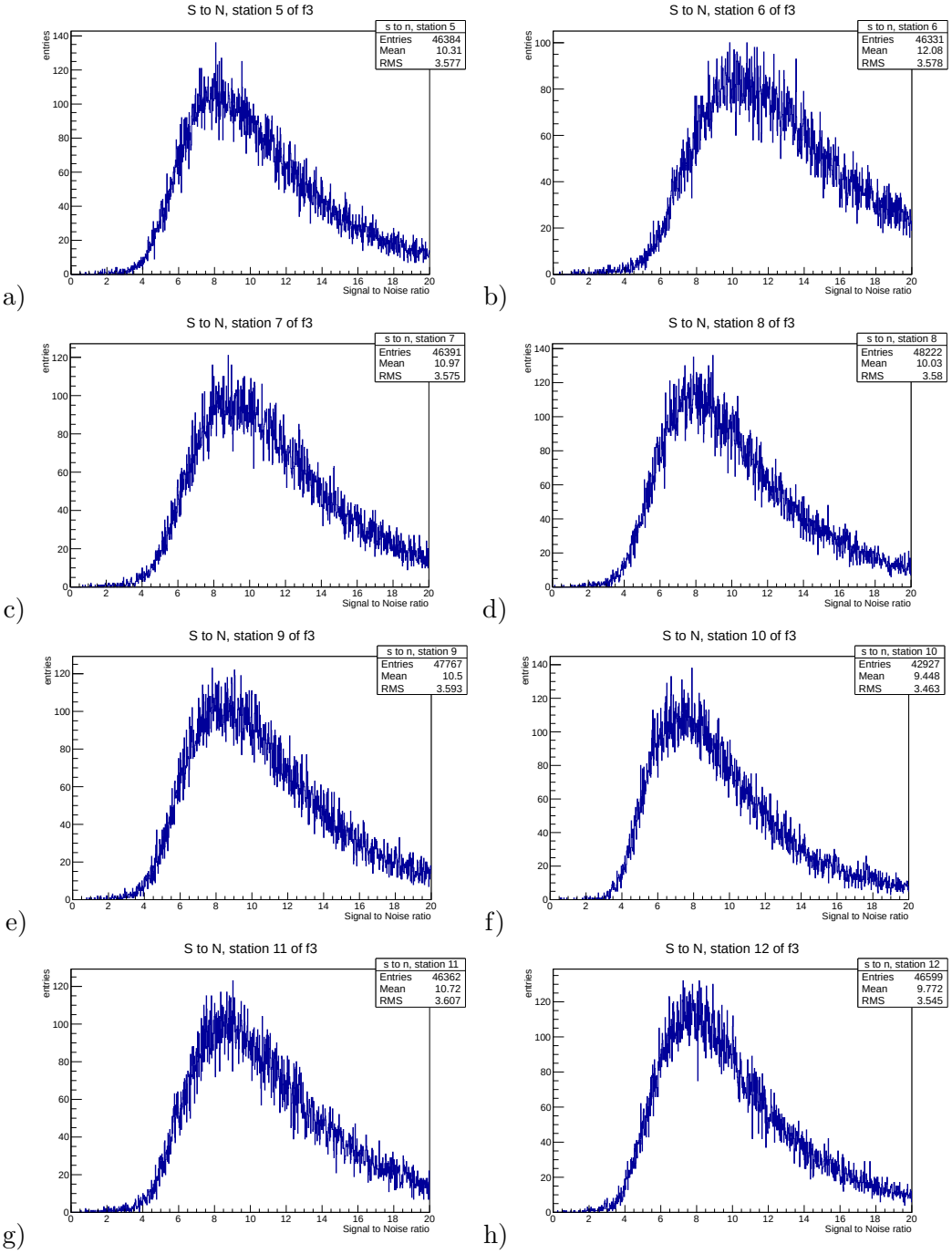

Figure 3.6: Signal to noise ratio S/N for frequency f3 for (a) detector 5, (b) detector 6, (c) detector 7, (d) detector 8, (e) detector 9, (f) detector 10, (g) detector 11, (h) detector 12.

frequency f_4

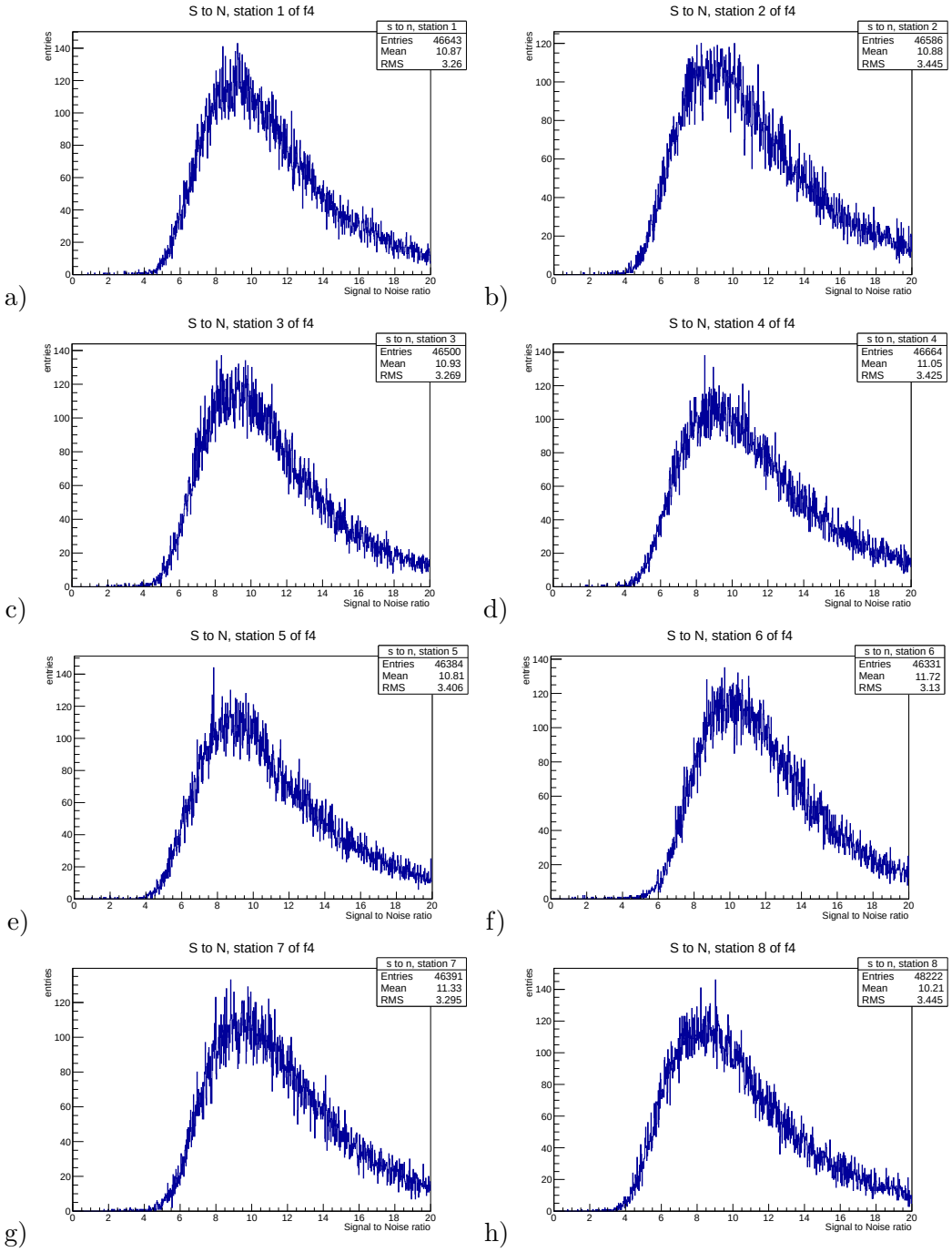

Figure 3.7: Signal to noise ratio S/N for frequency f4 for (a) detector 1, (b) detector 2, (c) detector 3, (d) detector 4, (e) detector 5, (f) detector 6, (g) detector 7, (h) detector 8.

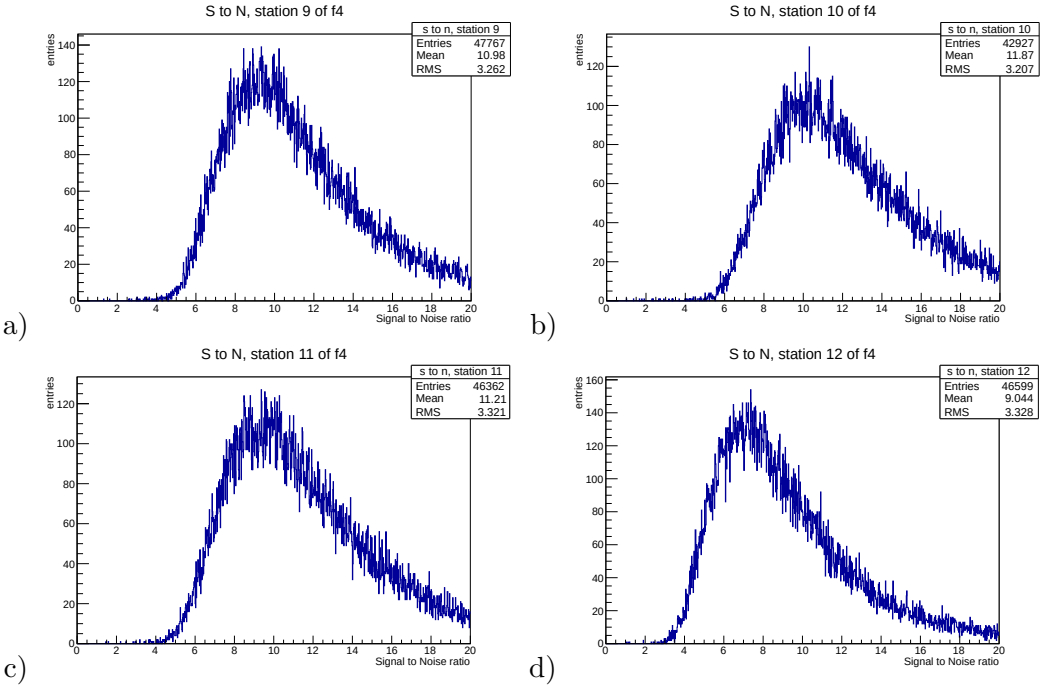

Figure 3.8: Signal to noise ratio S/N for frequency f4 for (a) detector 9, (b) detector 10, (c) detector 11, (d) detector 12.

frequency f_5

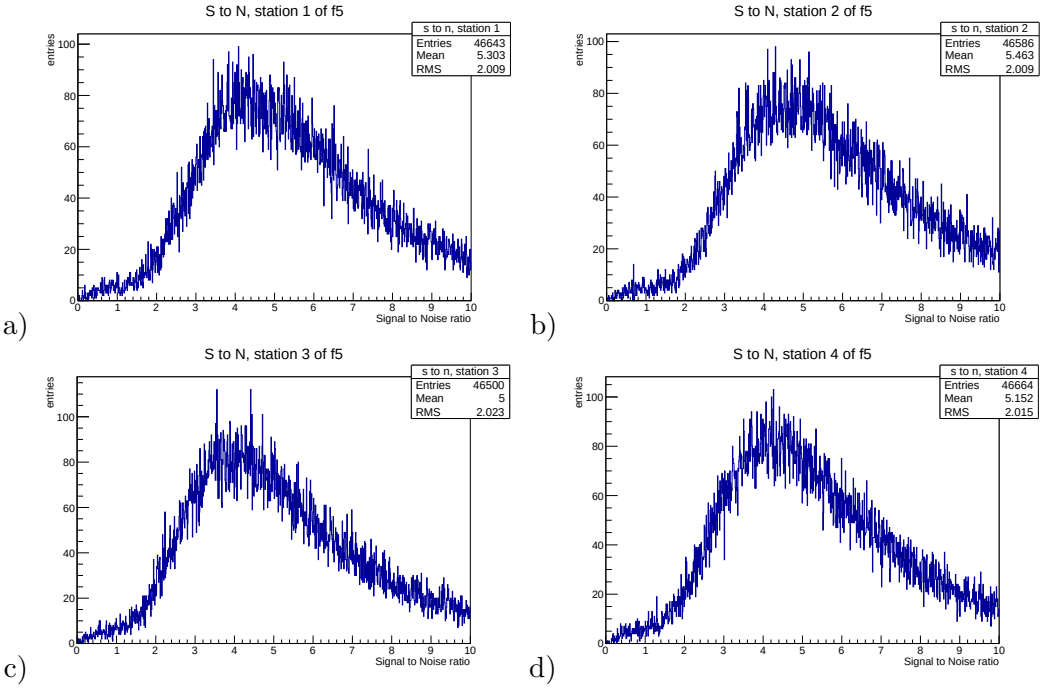

Figure 3.9: Signal to noise ratio S/N for frequency f5 for (a) detector 1, (b) detector 2, (c) detector 3, (d) detector 4.

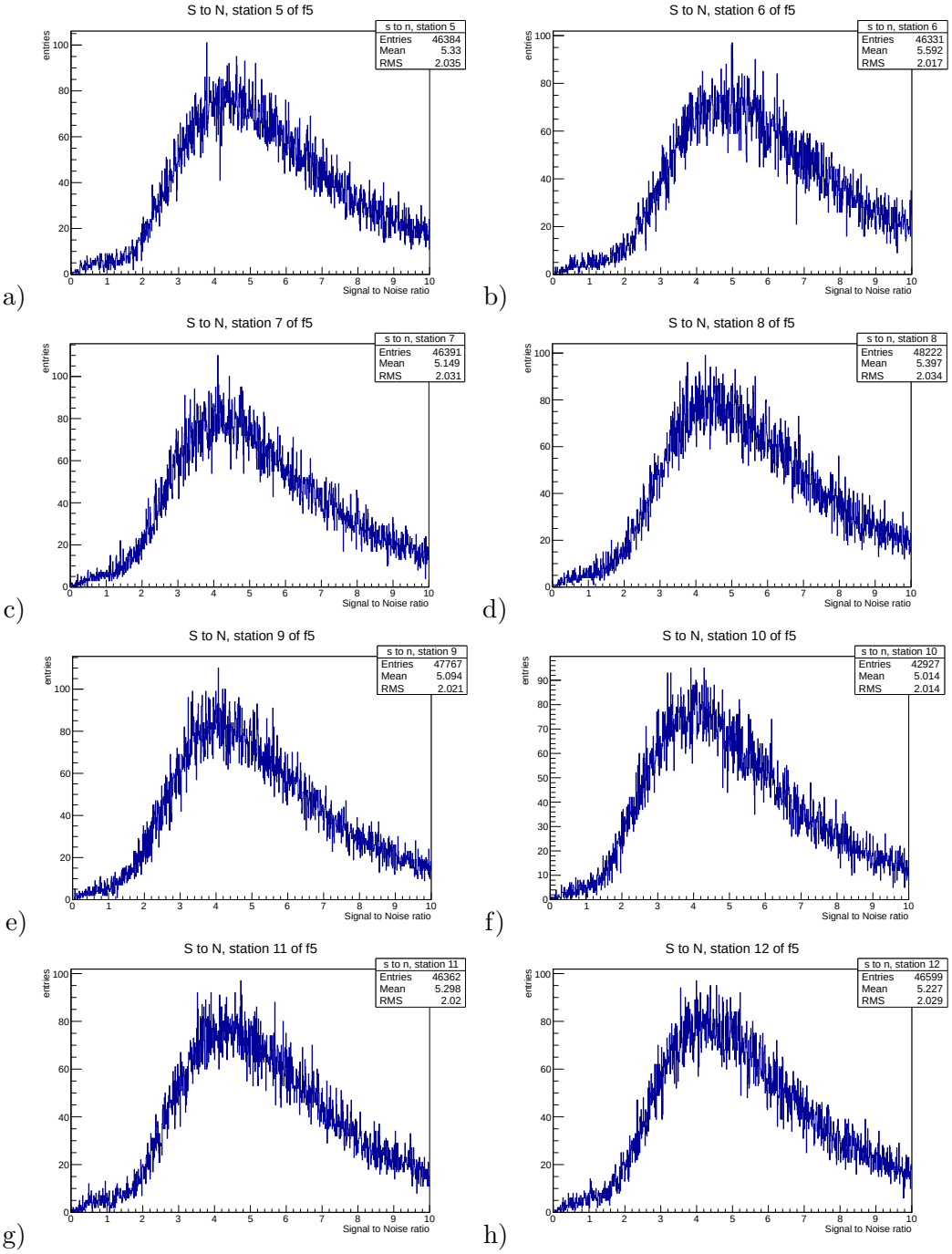

Figure 3.10: Signal to noise ratio S/N for frequency f5 for (a) detector 5, (b) detector 6, (c) detector 7, (d) detector 8, (e) detector 9, (f) detector 10, (g) detector 11, (h) detector 12.

3.3 Data

I used the following data set:

runnumber: 200270
startime: Saterday, 25th of February at 01:25 hour, 2012.
endtime: Thursday, 1st of March at 23.54 hour, 2012.

3.4 Amplitude in time

frequency f_2

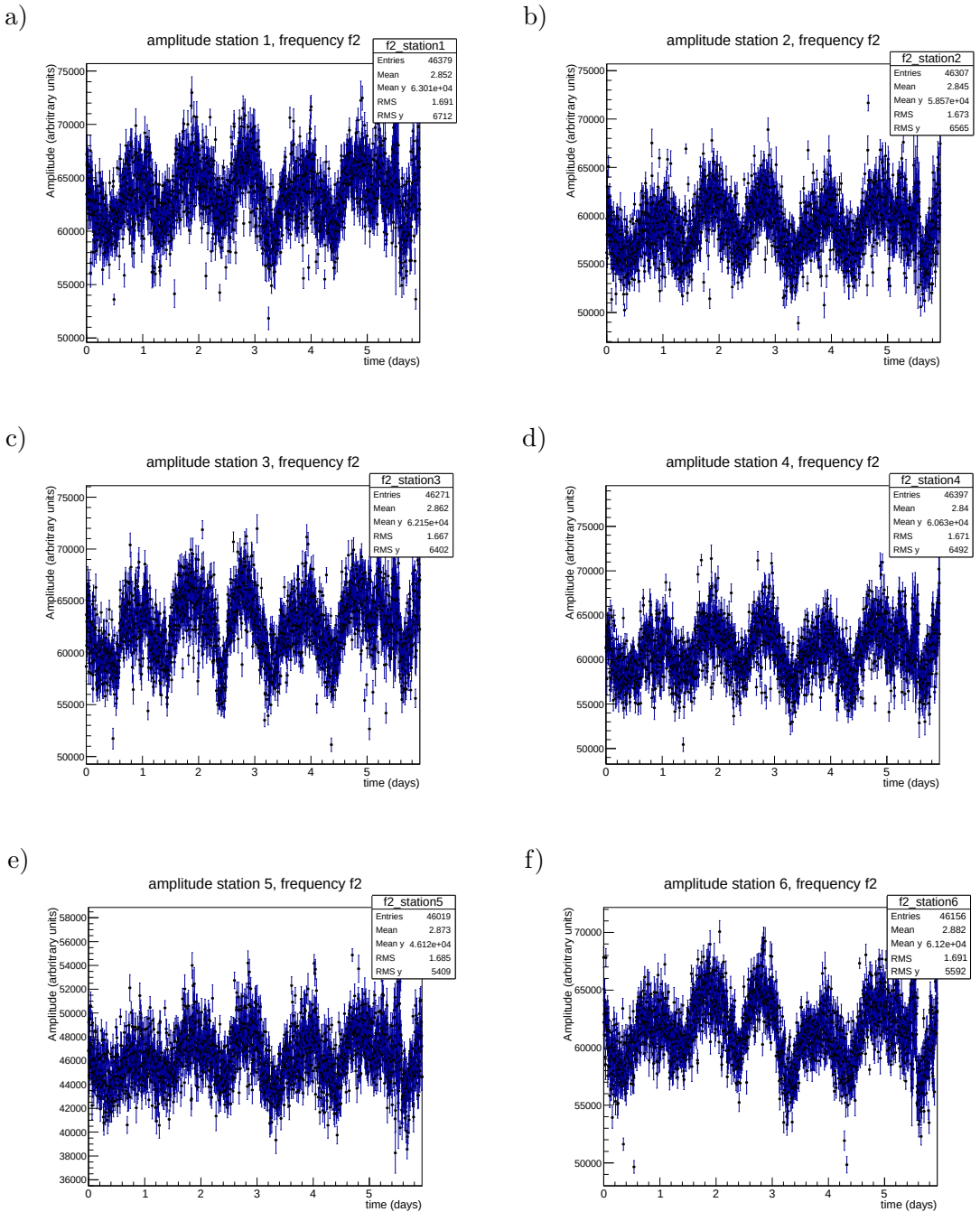

Figure 3.11: Amplitude against time for frequency f_2 for (a) detector 1, (b) detector 2, (c) detector 3, (d) detector 4, (e) detector 5, (f) detector 6.

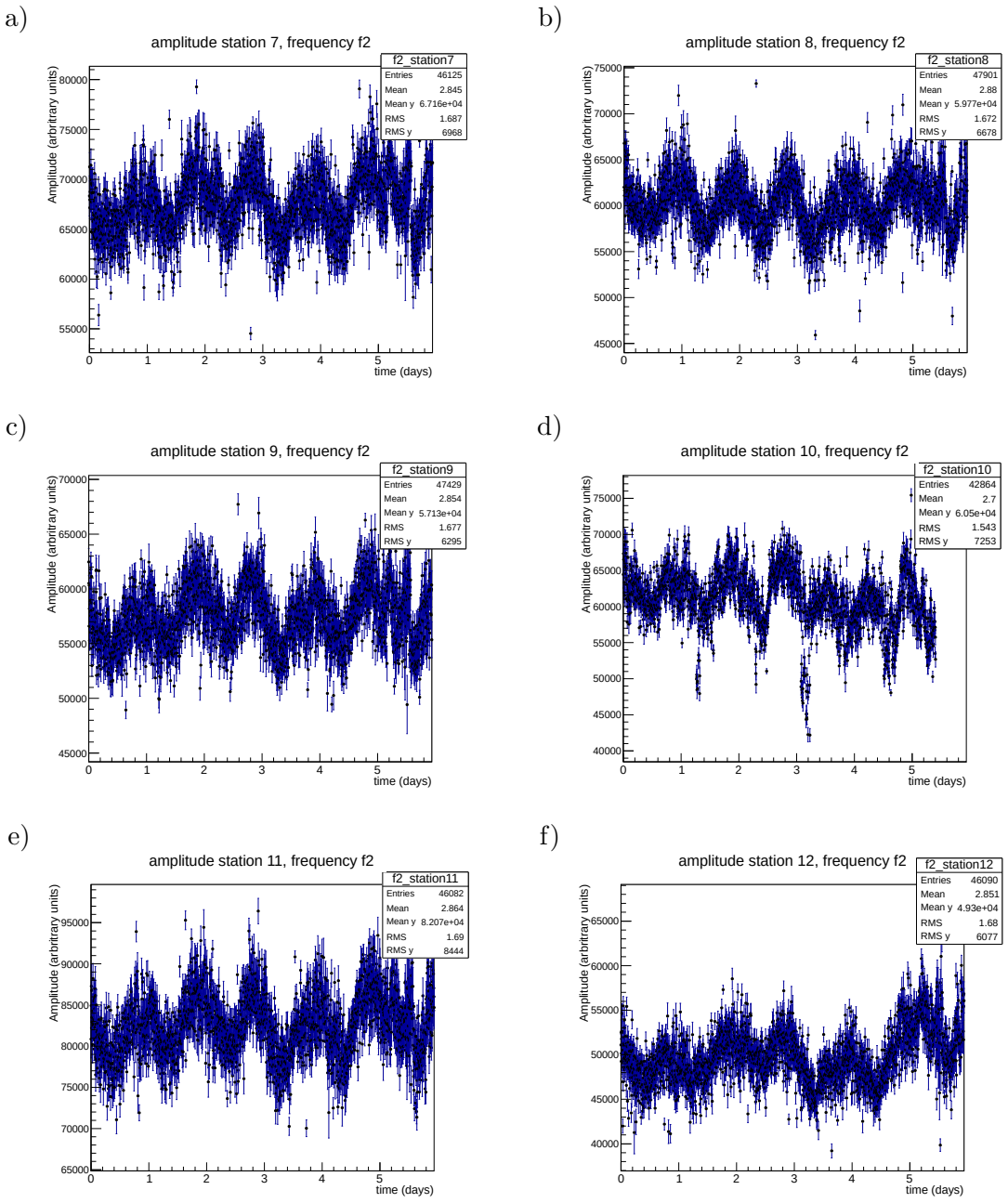

Figure 3.12: Amplitude against time for frequency f_2 for (a) detector 7, (b) detector 8, (c) detector 9, (d) detector 10, (e) detector 11, (f) detector 12.

frequency f_3

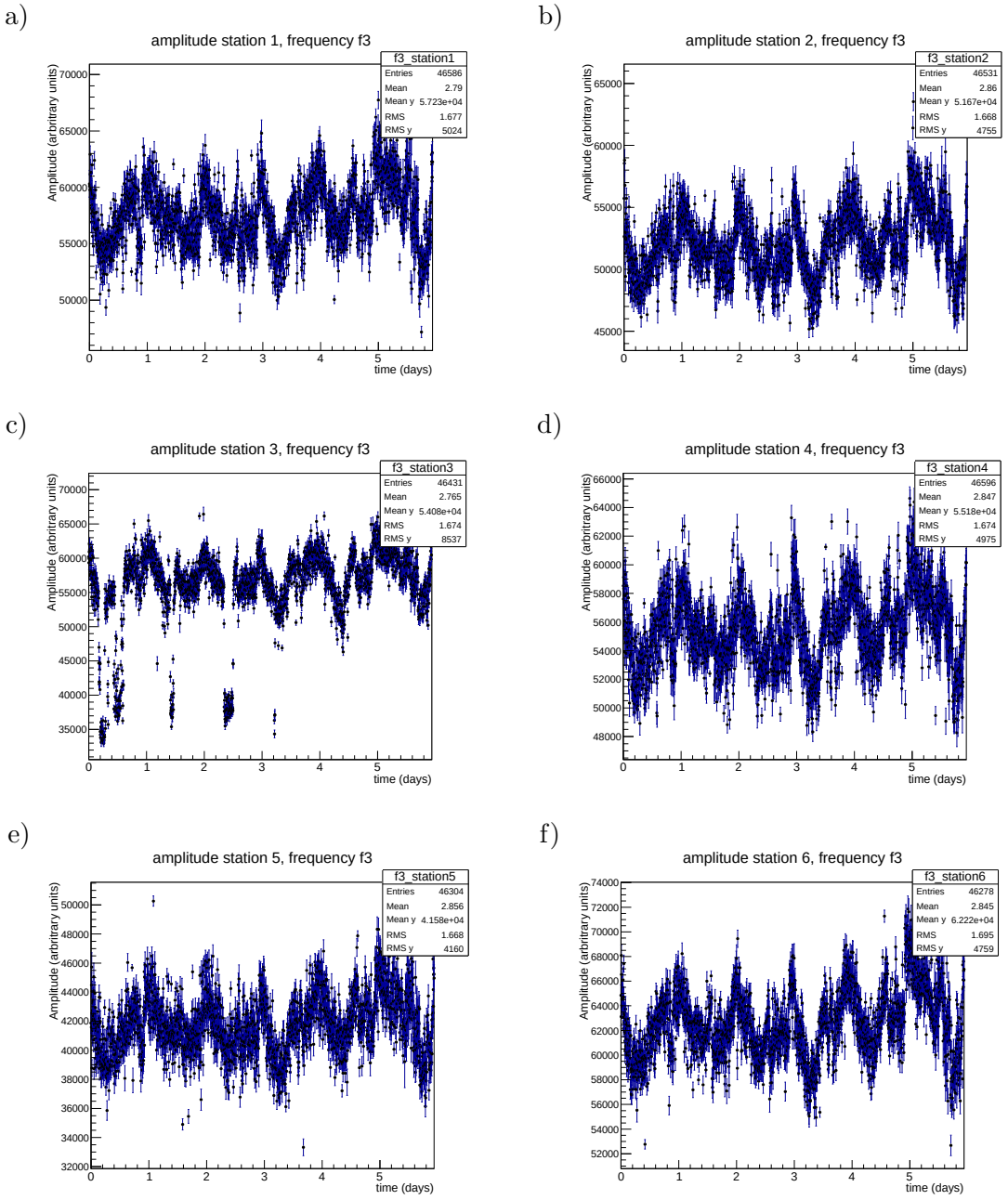

Figure 3.13: Amplitude against time for frequency f_3 for (a) detector 1, (b) detector 2, (c) detector 3, (d) detector 4, (e) detector 5, (f) detector 6.

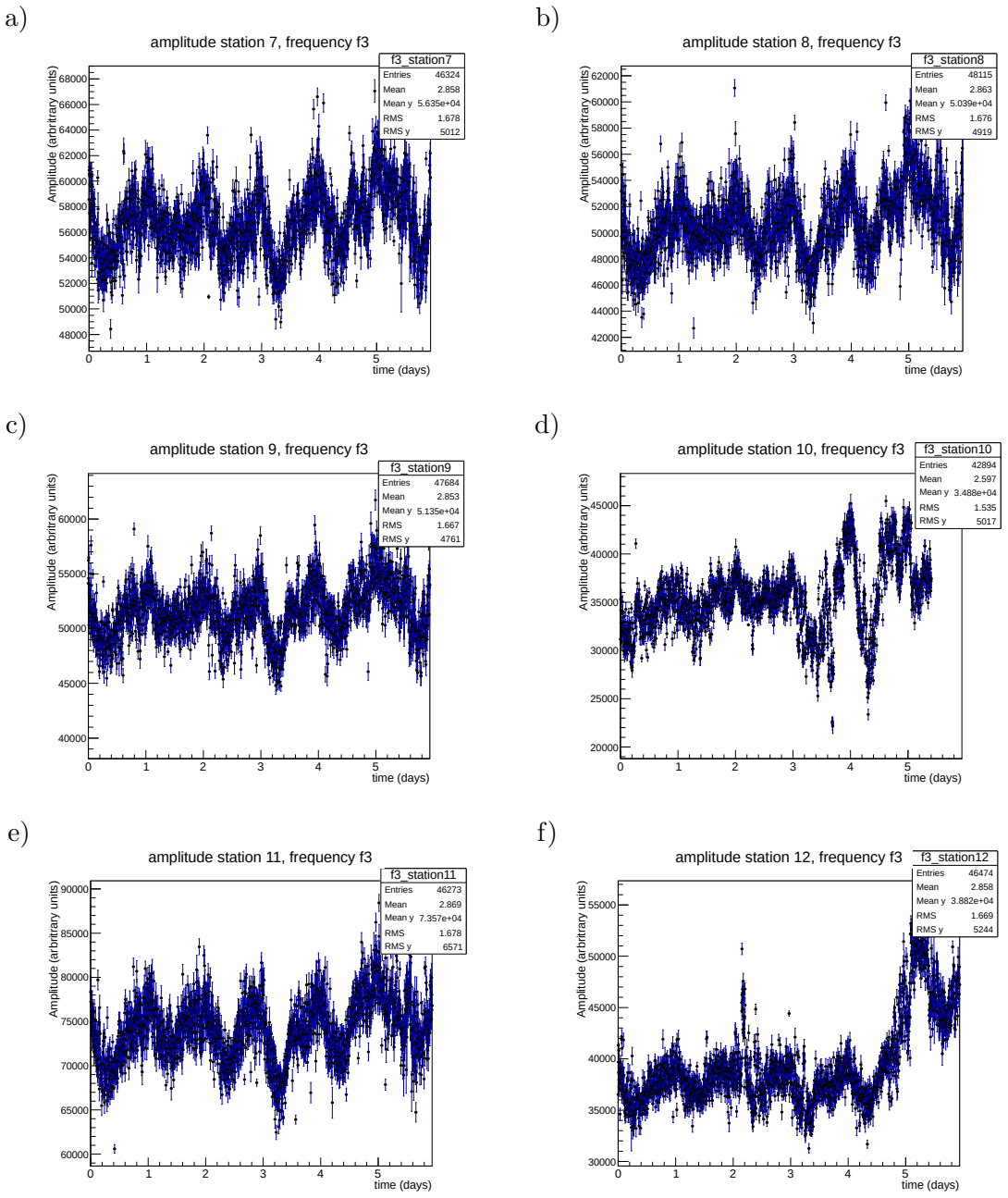

Figure 3.14: Amplitude against time for frequency f_3 for (a) detector 7, (b) detector 8, (c) detector 9, (d) detector 10, (e) detector 11, (f) detector 12.

frequency f_4

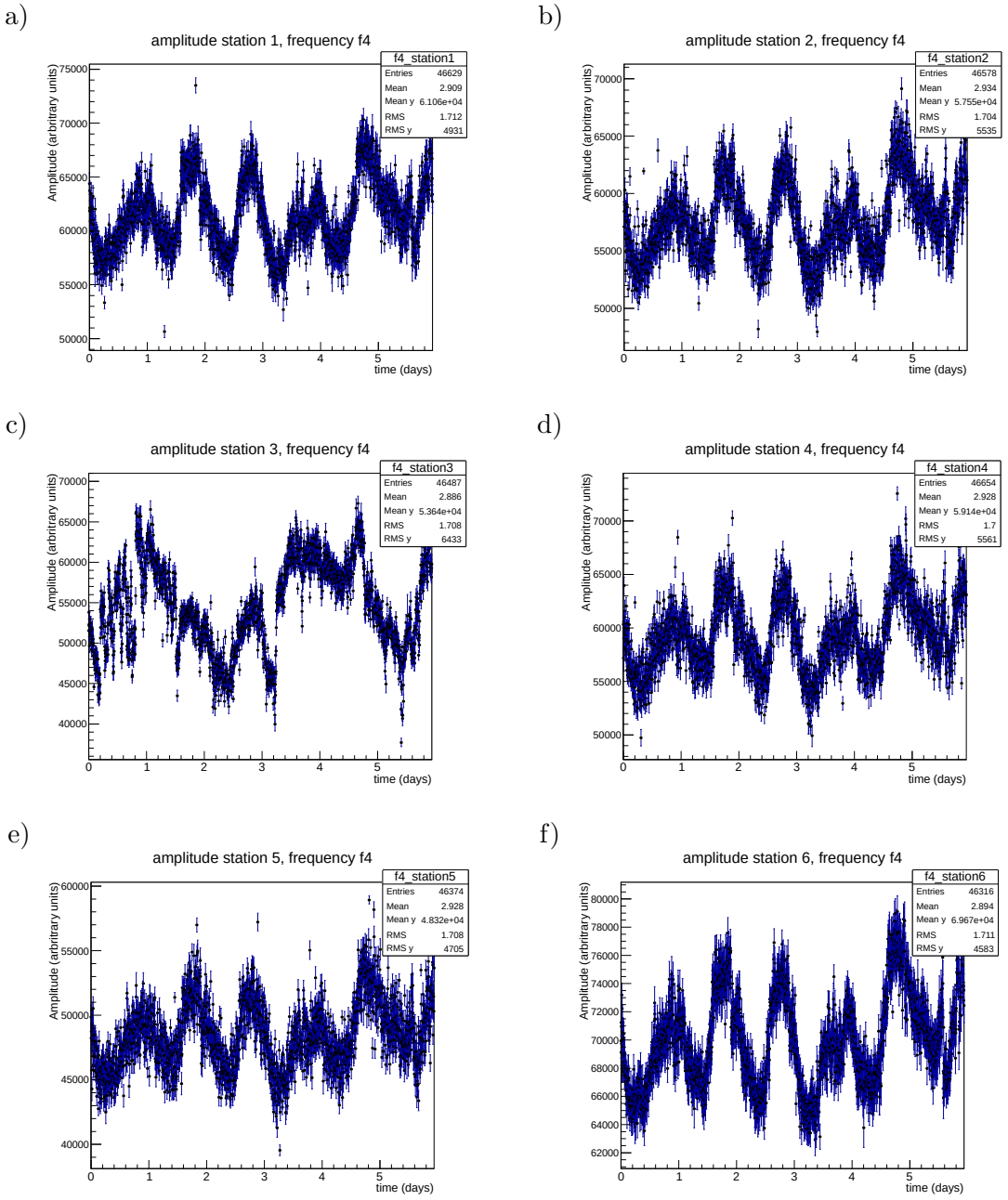

Figure 3.15: Amplitude against time for frequency f_4 for (a) detector 1, (b) detector 2, (c) detector 3, (d) detector 4, (e) detector 5, (f) detector 6.

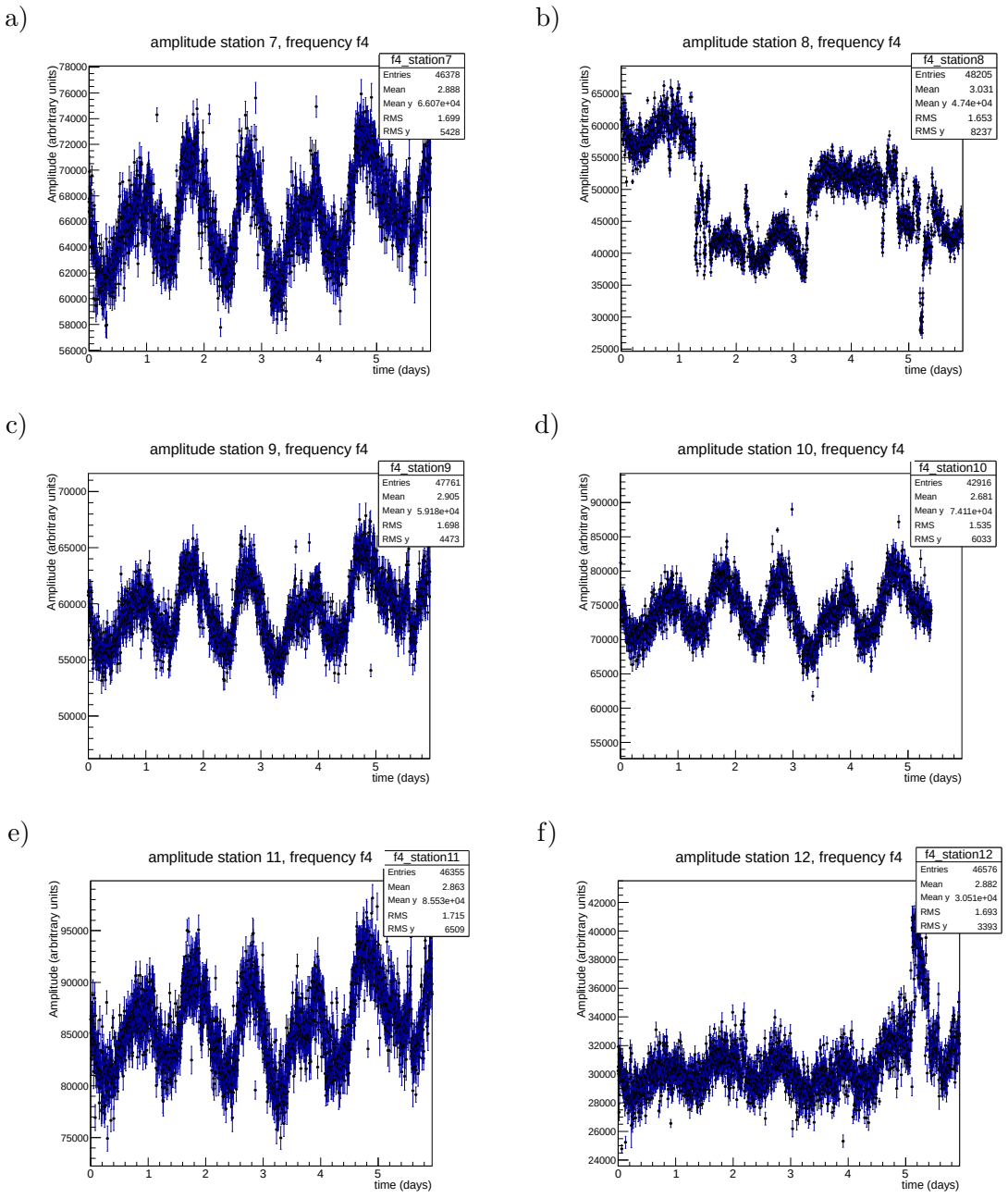

Figure 3.16: Amplitude against time for frequency f_4 for (a) detector 7, (b) detector 8, (c) detector 9, (d) detector 10, (e) detector 11, (f) detector 12.

3.5 Amplitude distribution with gaussian fit

frequency f_2

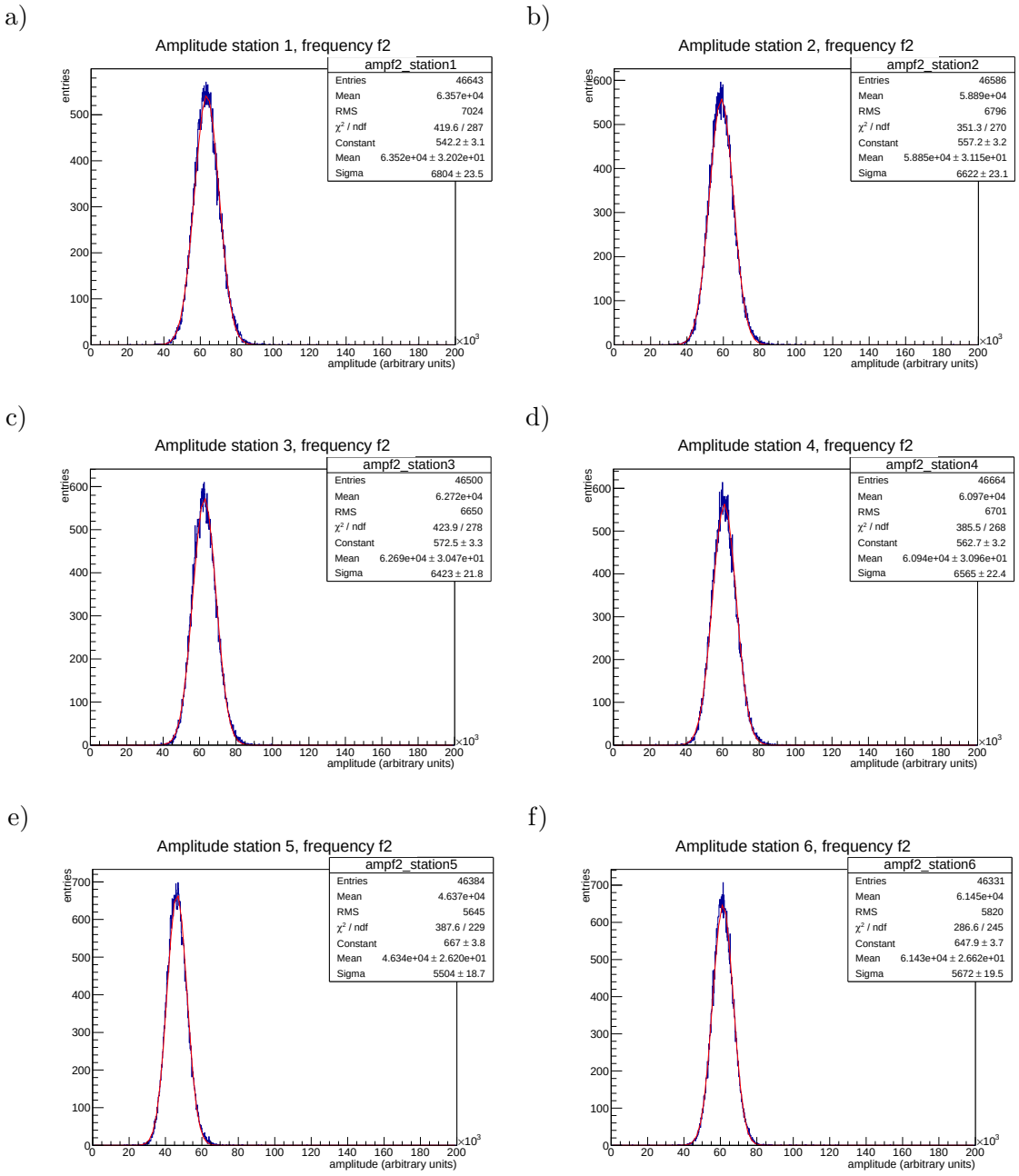

Figure 3.17: Distribution of the amplitude from frequency f_2 over 6 days of measuring for (a) detector 1, (b) detector 2, (c) detector 3, (d) detector 4, (e) detector 5, (f) detector 6.

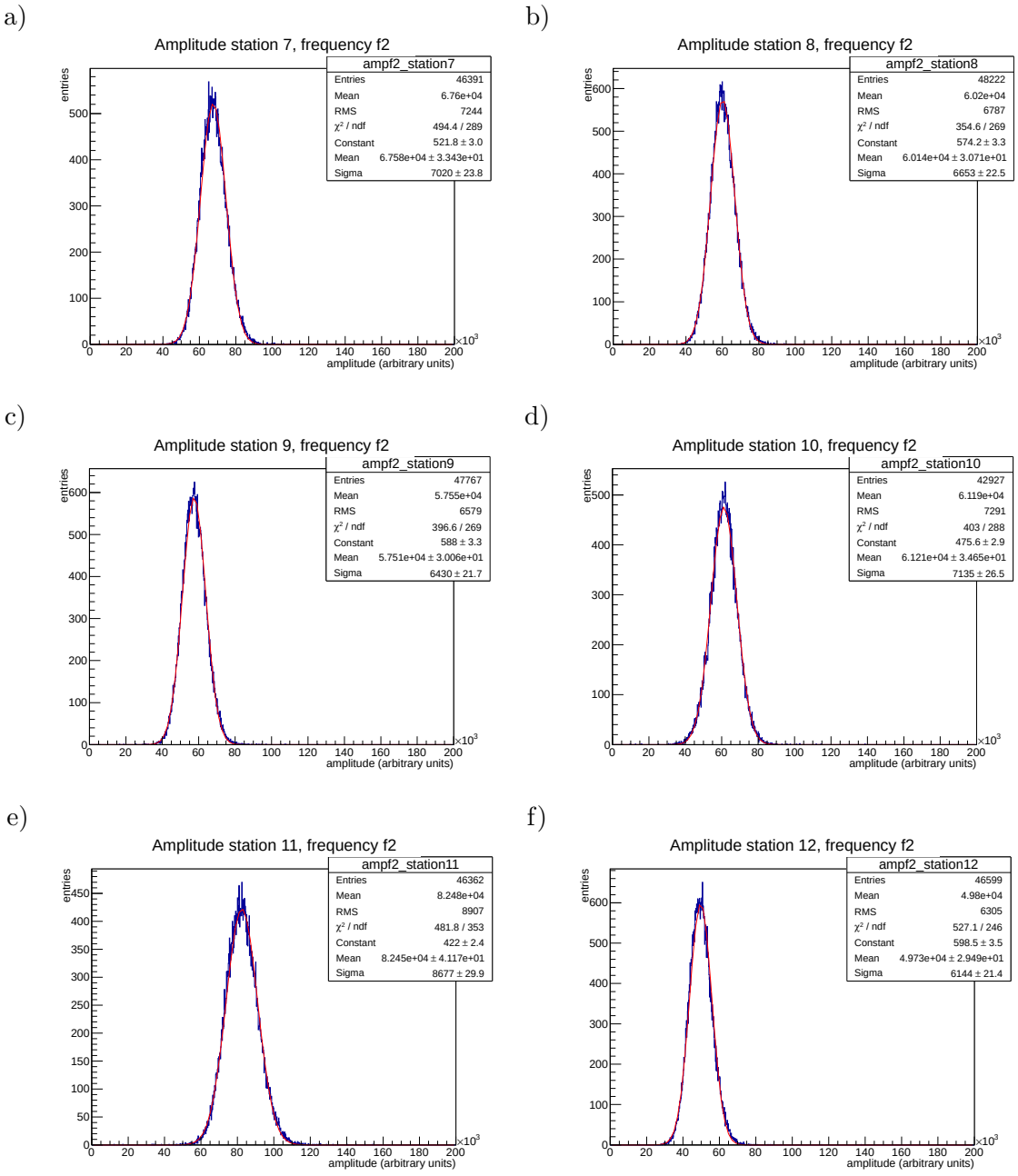

Figure 3.18: Distribution of the amplitude from frequency f_2 over 6 days of measuring for (a) detector 7, (b) detector 8, (c) detector 9, (d) detector 10, (e) detector 11, (f) detector 12.

frequency f_3

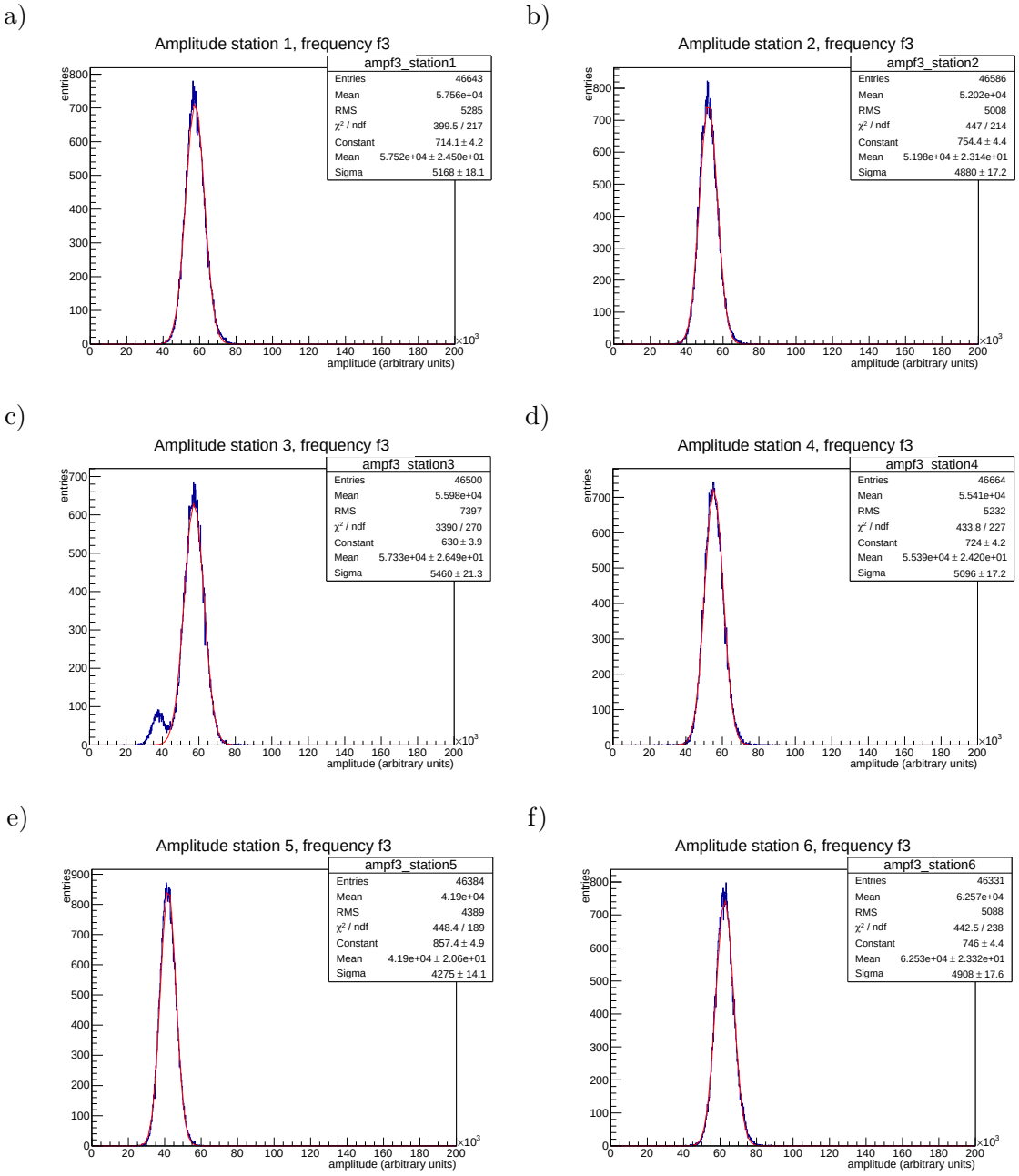

Figure 3.19: Distribution of the amplitude from frequency f_3 over 6 days of measuring for (a) detector 1, (b) detector 2, (c) detector 3, (d) detector 4, (e) detector 5, (f) detector 6.

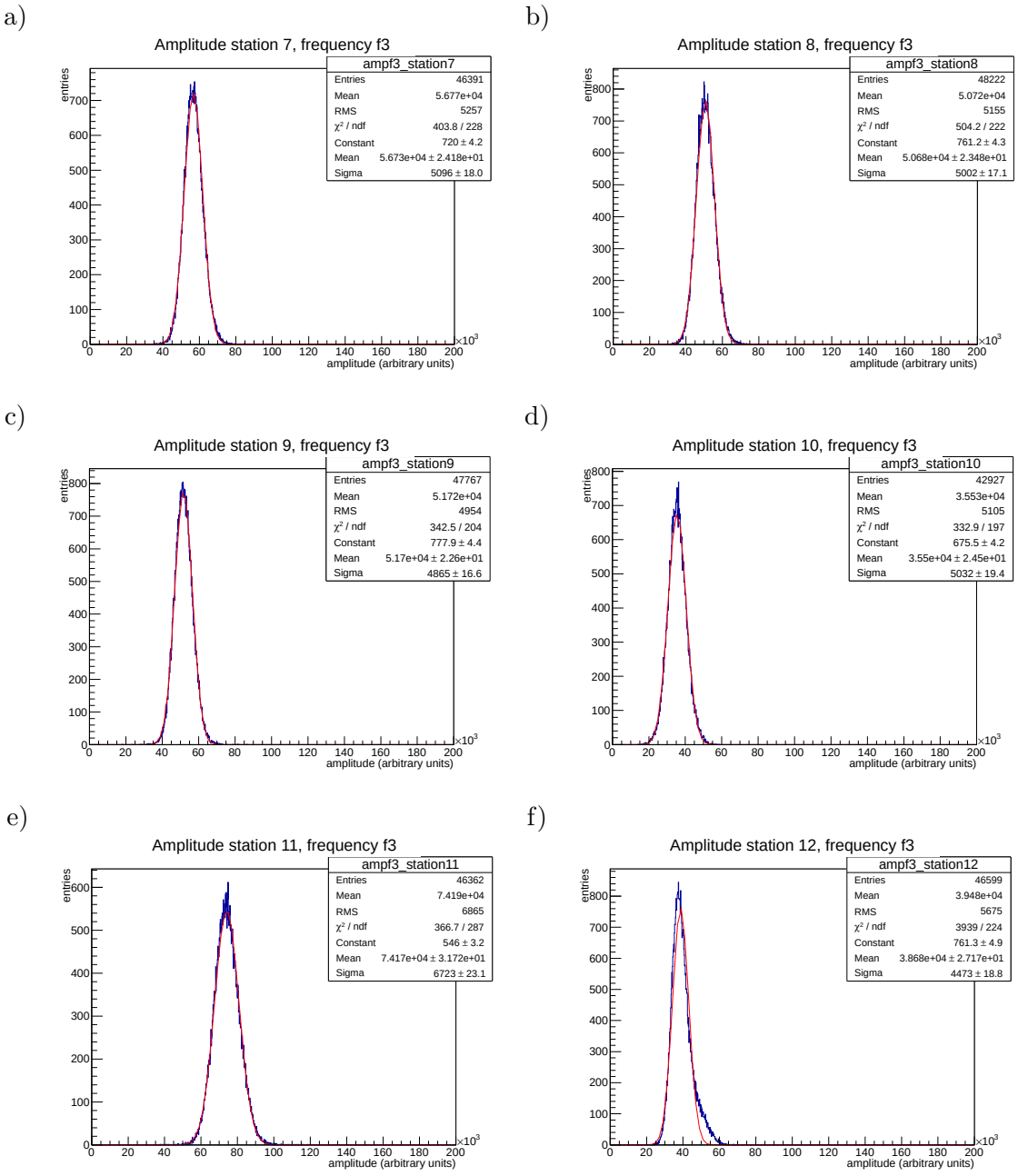

Figure 3.20: Distribution of the amplitude from frequency f_3 over 6 days of measuring for (a) detector 7, (b) detector 8, (c) detector 9, (d) detector 10, (e) detector 11, (f) detector 12.

frequency f_4

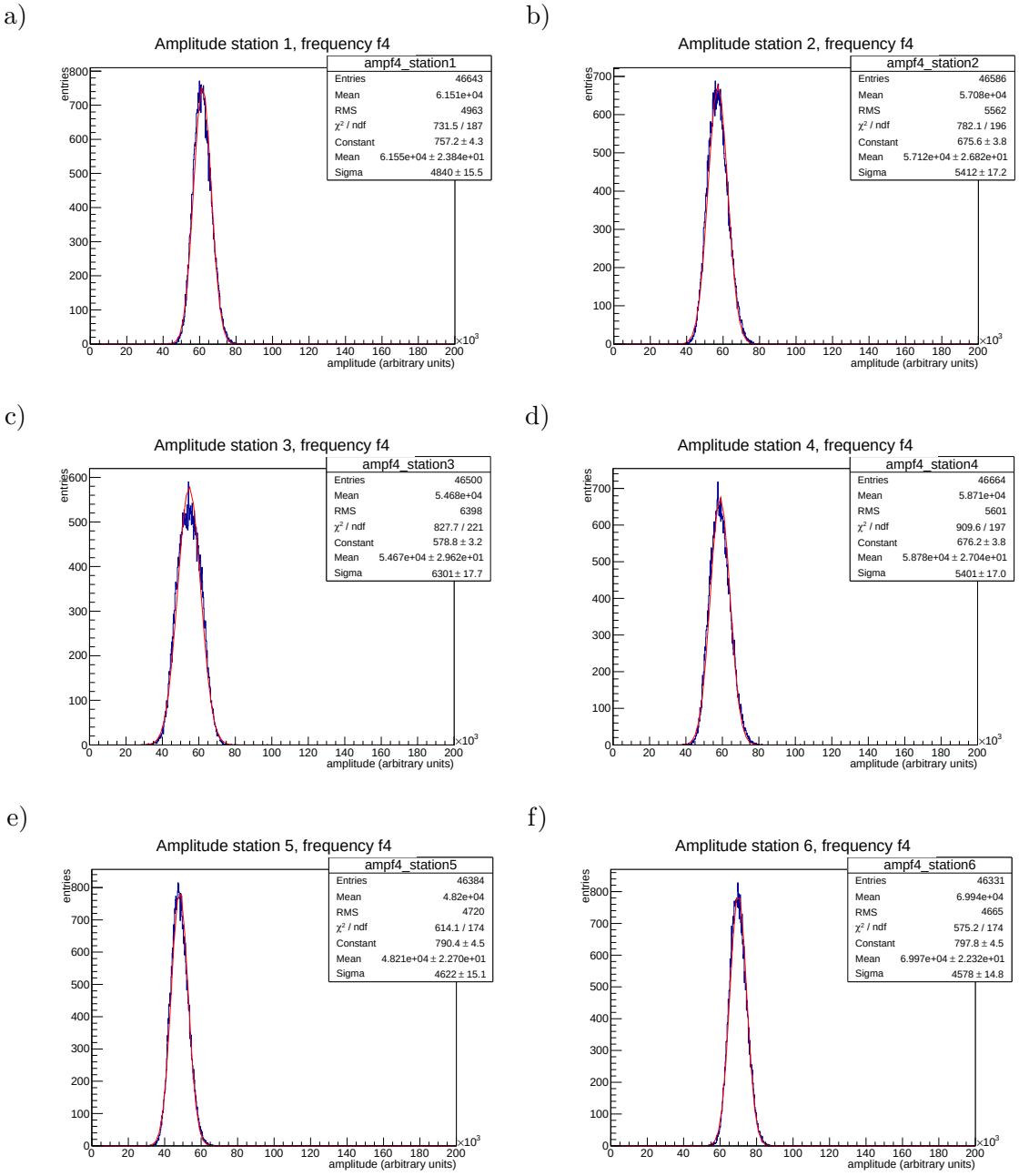

Figure 3.21: Distribution of the amplitude from frequency f_4 over 6 days of measuring for (a) detector 1, (b) detector 2, (c) detector 3, (d) detector 4, (e) detector 5, (f) detector 6.

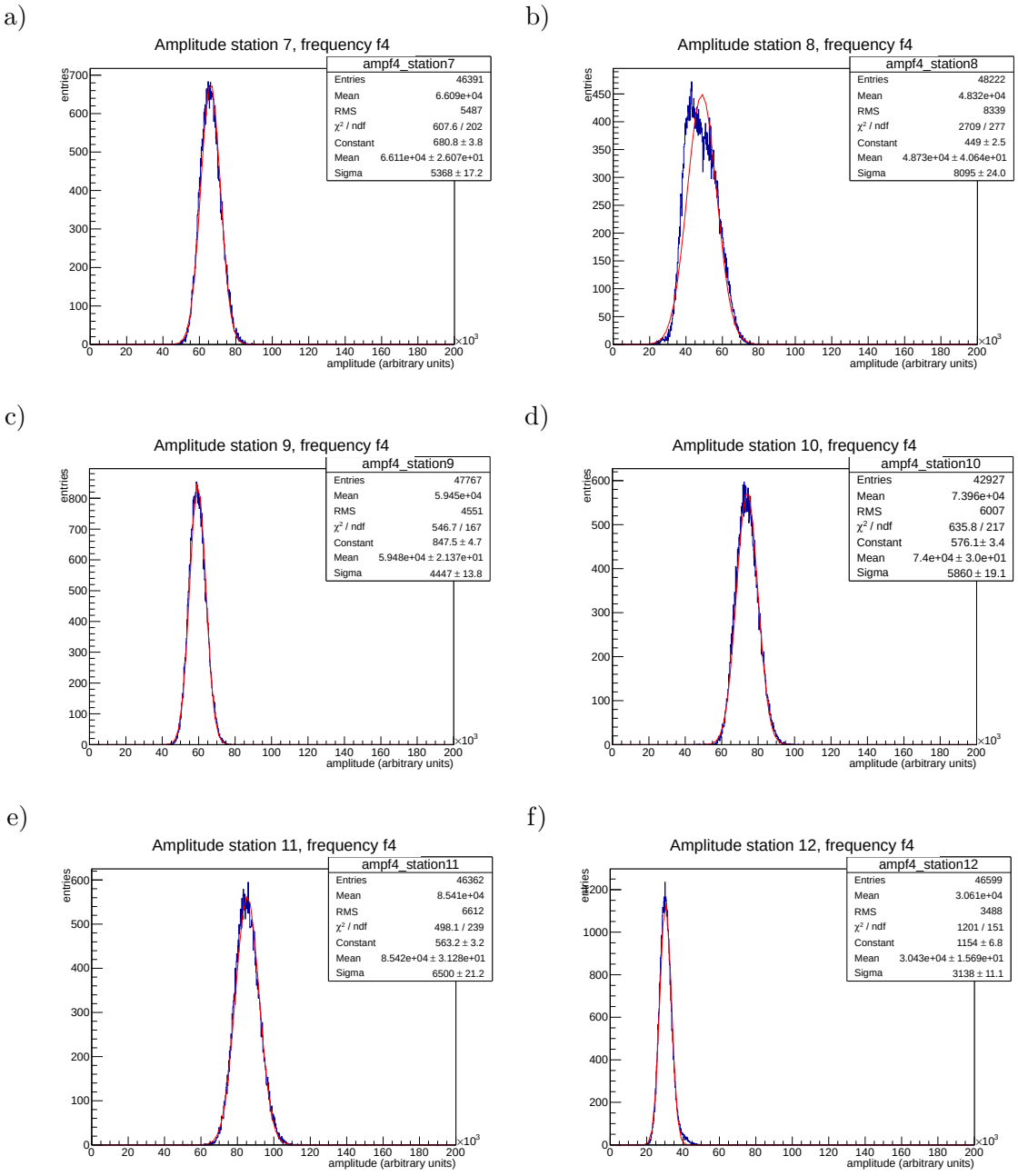

Figure 3.22: Distribution of the amplitude from frequency f_4 over 6 days of measuring for (a) detector 7, (b) detector 8, (c) detector 9, (d) detector 10, (e) detector 11, (f) detector 12.

3.6 Dector log

Beneath the detector log of April 18th:

18 April 2012

Maintenance of the LPDA antennas:

It was found in March 2012 that the attachement of a few dipoles to the outer wiring of the LPDAs broke at altogether 13 stations. As a consequence the dipoles were not aligned in a proper way anymore. To clear these issue Jonny Kleinfeller and I started a maintenance campaign in the first week of April. During this procedure we removed the antennas from the pole and replaced the attachement of each of the 32 dipoles (not only the broken ones). Afterwards the antennas were attached to the pole again and aligned exactly as before the removal. This took 2 hours for each antenna. The stations should have recorded only noise traces during this time. The downtime of each station is denoted in the table below.

AERA station Id	downtime [date / local time]	number of broken dipoles
1	25.4 / 14:40 - 16:10	0
2	11.4 / 11:40 - 13:40	2
3	10.4 / 15:30 - 17:30	2
4	24.4 / 15:30 - 17:30	0
5	24.4 / 11:30 - 13:30	0
6	10.4 / 12:00 - 14:00	1
7	25.4 / 13:30 - 14:40	0
8	6.4 / 15:15 - 17:15	1
9	24.4 / 13:30 - 15:30	0
10	10.4 / 13:50 - 15:50	5
11	4.5 / 12:00 - 13:00	0
12	11.4 / 13:45 - 15:45	1
13	25.4 / 11:30 - 13:15	0
14	4.5 / 13:15 - 14:15	0
15	12.4 / 14:55 - 16:55	0
16	9.4 / 12:10 - 14:10	7
17	4.5 / 14:30 - 15:45	0
18	12.4 / 11:05 - 13:05	0
19	11.4 / 15:30 - 17:30	1
20	9.4 / 16:10 - 10.4 / 12:15	2
21	12.4 / 13:10 - 15:10	0
22	9.4 / 14:05 - 16:05	2
23	6.4 / 11:00 - 13:00	5
24	6.4 / 13:15 - 15:15	1

Klaus Weidenhaupt